Title

Exercise Intolerance in Heart Failure With Preserved Ejection Fraction

Journal

Circulation, 137(2)

ISSN

0009-7322

Authors

Houstis, Nicholas E

Eisman, Aaron S

Pappagianopoulos, Paul P

et al.

Publication Date

2018-01-09

DOI

10.1161/circulationaha.117.029058

Peer reviewed

Exercise Intolerance in Heart Failure With Preserved Ejection Fraction

Diagnosing and Ranking Its Causes Using Personalized O_2 Pathway Analysis

Editorial, see p 162

BACKGROUND: Heart failure with preserved ejection fraction (HFpEF) is a common syndrome with a pressing shortage of therapies. Exercise intolerance is a cardinal symptom of HFpEF, yet its pathophysiology remains uncertain.

METHODS: We investigated the mechanism of exercise intolerance in 134 patients referred for cardiopulmonary exercise testing: 79 with HFpEF and 55 controls. We performed cardiopulmonary exercise testing with invasive monitoring to measure hemodynamics, blood gases, and gas exchange during exercise. We used these measurements to quantify 6 steps of oxygen transport and utilization (the O_2 pathway) in each patient with HFpEF, identifying the defective steps that impair each one's exercise capacity (peak $\dot{V}o_2$). We then quantified the functional significance of each O_2 pathway defect by calculating the improvement in exercise capacity a patient could expect from correcting the defect.

RESULTS: Peak $\dot{V}o_2$ was reduced by 34±2% (mean±SEM, $P<0.001$) in HFpEF compared with controls of similar age, sex, and body mass index. The vast majority (97%) of patients with HFpEF harbored defects at multiple steps of the O_2 pathway, the identity and magnitude of which varied widely. Two of these steps, cardiac output and skeletal muscle O_2 diffusion, were impaired relative to controls by an average of 27±3% and 36±2%, respectively ($P<0.001$ for both). Due to interactions between a given patient's defects, the predicted benefit of correcting any single one was often minor; on average, correcting a patient's cardiac output led to a 7±0.5% predicted improvement in exercise intolerance, whereas correcting a patient's muscle diffusion capacity led to a 27±1% improvement. At the individual level, the impact of any given O_2 pathway defect on a patient's exercise capacity was strongly influenced by comorbid defects.

CONCLUSIONS: Systematic analysis of the O_2 pathway in HFpEF showed that exercise capacity was undermined by multiple defects, including reductions in cardiac output and skeletal muscle diffusion capacity. An important source of disease heterogeneity stemmed from variation in each patient's personal profile of defects. Personalized O_2 pathway analysis could identify patients most likely to benefit from treating a specific defect; however, the system properties of O_2 transport favor treating multiple defects at once, as with exercise training.

Nicholas E. Houstis, MD, PhD
Aaron S. Eisman, BS
Paul P. Pappagianopoulos, MEd
Luke Wooster, BA
Cole S. Bailey, BA
Peter D. Wagner, MD
Gregory D. Lewis, MD

Correspondence to: Gregory D. Lewis, MD, Heart Failure and Cardiac Transplantation Unit, Massachusetts General Hospital, Bigelow 800, 55 Fruit St, Boston, MA 02114. E-mail glewis@partners.org

Sources of Funding, see page 159

Key Words: cardiac output ■ comorbidity ■ diagnosis ■ diffusion ■ microcirculation ■ systems biology ■ taxonomy

Clinical Perspective

What Is New?

- Systematic quantification of the oxygen transport and utilization cascade (O_2 pathway) revealed extensive variation in the mechanisms of exercise intolerance among patients with heart failure with preserved ejection fraction.
- Impaired skeletal muscle diffusion capacity was found to be an important peripheral cause of exercise intolerance.
- The vast majority of patients harbored compound mechanisms of exercise intolerance, defined as ≥2 defective steps in the O_2 pathway.
- The predicted improvement in exercise capacity attributable to correcting any single O_2 pathway defect was constrained by interactions with comorbid defects.

What Are the Clinical Implications?

- The importance of impaired peripheral O_2 extraction to exercise intolerance in heart failure with preserved ejection fraction highlights the need to develop widely applicable tools for diagnosing peripheral abnormalities during exercise.
- A taxonomy of heart failure with preserved ejection fraction should account for the diversity of underlying mechanisms of disease.
- The efficacy of treating any individual O_2 pathway step such as cardiac output will depend on a patient's comorbid O_2 pathway abnormalities.

Despite repeated attempts, no large trial of medical therapy for heart failure with preserved ejection fraction (HFpEF) has met its primary end point. Two entangled challenges have contributed to this impasse: uncertainty in the pathophysiology and heterogeneity of the patient population. The dominant theory of HFpEF pathophysiology has been impaired cardiac relaxation,[1] but it now competes with several rivals.[2–6] The inconvenient reality may be that no single mechanism accounts for symptoms in all patients. Splitting the umbrella diagnosis of HFpEF into mechanism-based subtypes would facilitate the identification, testing, and ultimately personalization of novel therapies.[7]

Exercise intolerance is a cardinal symptom of HFpEF, one whose distinct etiologies could be the basis of a disease taxonomy. A useful system for organizing these etiologies springs from 1 central relationship, the dependence of exercise performance on oxygen (O_2) consumption.[8] Exercise capacity can be formally defined as the rate of O_2 consumption ($\dot{V}o_2$) at peak exercise. Any factor that limits peak $\dot{V}o_2$, by impeding O_2 delivery or utilization, can be said to cause exercise intolerance. O_2 delivery and utilization are in turn determined by a series of steps akin to a bucket brigade that transport O_2 from the mouth all the way to respiring mitochondria. The main steps in this O_2 cascade include alveolar ventilation, diffusion from alveolar gas into pulmonary capillary blood and loading onto hemoglobin, convective transport by the heart (cardiac output) and vasculature to the peripheral microcirculation, diffusion into skeletal muscle, and mitochondrial respiration: in aggregate, the O_2 pathway (Figure 1).[9] The cause of exercise intolerance in HFpEF has been classically attributed to a defect in 1 step, cardiac output,[1,10] but the growing recognition of extracardiac abnormalities[6,11,12] underscores the need to characterize the entire O_2 pathway. Many O_2 pathway steps can be quantified by using invasively monitored cardiopulmonary exercise testing. Once quantified, a patient's mechanism of exercise intolerance can be discretized into a list of defective steps, eg, impaired cardiac output and anemia. This list of causal O_2 pathway defects personalizes a diagnosis of exercise intolerance much as a genotype of tumor driver mutations personalizes a diagnosis of cancer.

Expressing exercise intolerance in terms of O_2 pathway defects is not only valuable for diagnosis, but also

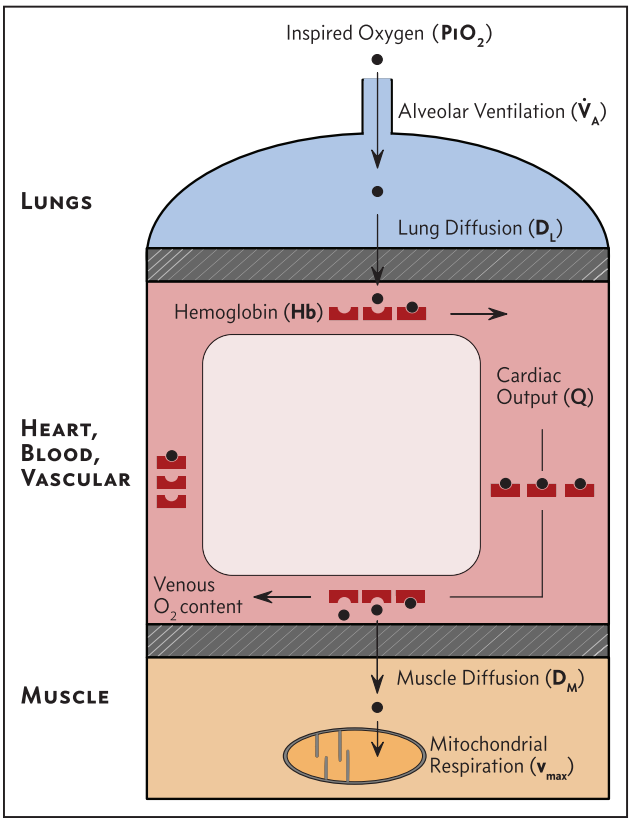

Figure 1. The O_2 pathway.
A schematic depicting the sequence of O_2 transport and utilization steps from mouth to mitochondria. D_L indicates lung diffusion capacity for O_2; D_M, skeletal muscle diffusion capacity for O_2; Hb, hemoglobin concentration; PIO_2, partial pressure of inspired O_2; Q, cardiac output; $\dot{V}A$, alveolar ventilation; and v_{max}, mitochondrial respiration capacity.

raises the prospect of targeting them for therapy. A defect's appeal as a target, however, depends on the magnitude of its causal impact on exercise capacity. This impact can be quantified as the improvement in peak $\dot{V}o_2$ that would result from fully correcting the defect. For example, discovering that a patient's cardiac output is depressed invites the question, just how much would the patient's exercise capacity improve if cardiac output were restored? The ability to answer this question could prove vital to the success of cardiac output therapies, but few tools exist to address it. The central challenge is that the answer could be highly context-dependent. If depressed cardiac output were the patient's only O_2 pathway defect, then the outcome of treating it would be self-evident: fully restoring cardiac output should fully correct exercise capacity. If, however, cardiac output were one of several O_2 pathway defects, interactions between them could impede the $\dot{V}o_2$ response to cardiac output therapy. Two patients with precisely the same cardiac output defect, but distinct sets of accessory O_2 pathway defects, could experience very different responses to therapy. This differential sensitivity to therapy caused by O_2 pathway background would be analogous to the variable penetrance of a pathological gene mutation caused by genetic background.

Here we sought to quantify the steps of O_2 transport from mouth to mitochondria, at the highest resolution to date in HFpEF. We also sought to quantify, for the first time, the relative importance of each of a patient's causal defects. Achieving these goals could enable new taxonomies of HFpEF as well as new paradigms for personalizing therapy. Finally, peak $\dot{V}o_2$ is a potent predictor of survival in HFpEF,[13] further highlighting the value of systematically quantifying its determinants.

METHODS

Patients

Our study population was drawn from consecutive patients referred to the Massachusetts General Hospital from 2006 to 2016 for chronic New York Heart Association II to IV symptoms, who underwent cardiopulmonary exercise testing with invasive hemodynamic monitoring. Patients with HFpEF were identified from this retrospective series by the following criteria: (1) chronic New York Heart Association II to IV symptoms; (2) an explicit cutoff for reduced exercise capacity, namely peak $\dot{V}o_2 \leq 80\%$ of predicted on the basis of age, sex, and height[14]; (3) preserved left ventricular ejection fraction, ≥0.50; and (4) a hemodynamic criterion for heart failure,[15,16] namely a pulmonary arterial wedge pressure ≥15 mm Hg at rest while supine, or alternatively a peak exercise pulmonary arterial wedge pressure ≥25 mm Hg. Individuals from the same referral series were assigned to the control group if they demonstrated normal exercise capacity, peak $\dot{V}o_2 \geq 90\%$ of predicted, and objective evidence of normal cardiovascular function by multiple measures: (1) left ventricular ejection fraction ≥0.50, and (2) supine resting pulmonary arterial wedge pressure <15 mm Hg. There was partial overlap between the patients with HFpEF studied here and those from our prior study (24/79 patients).[6]

Patients were excluded from analysis if they met any of the following criteria: (1) incomplete pulmonary arterial catheter measurements, (2) submaximal exercise as evidenced by peak respiratory exchange ratio <1.0, (3) age <40 years, (4) documented intracardiac shunting, (5) severe valvular heart disease, (6) flow-limiting coronary artery disease, and (7) arterial O_2 saturation <90% at peak exercise. This study was approved by the Partners Healthcare Institutional Review Board, and all patients gave informed consent. The authors had full access to the data and take responsibility for its integrity and for the article as written.

Cardiopulmonary Exercise Testing

All patients performed maximal incremental upright cycle ergometry with a pulmonary arterial catheter placed in the internal jugular vein and a systemic arterial catheter placed in the radial artery. Left ventricular ejection fraction was assessed either by resting echocardiography or resting ventriculography. Further testing details are described in the Methods in the online-only Data Supplement.

O_2 Pathway Analysis

Six steps of the O_2 pathway were quantified at peak exercise (Figure 1): alveolar ventilation ($\dot{V}_A$), lung diffusion capacity for O_2 (D_L), cardiac output (Q), hemoglobin concentration (Hb), skeletal muscle diffusion capacity for O_2 (D_M), and mitochondrial oxidative phosphorylation capacity (v_{max}). The term O_2 extraction refers to the removal of O_2 from tissue capillary blood by pathway steps such as diffusion and mitochondrial respiration. We refer to the O_2-extracting compartment as a whole as the periphery. O_2 pathway parameters were estimated by solving the governing equations for O_2 transport and utilization[17] (Table I and Algorithm 1 in the online-only Data Supplement). To estimate a patient's O_2 pathway parameters from these equations, peak exercise measurements were used as inputs, and the parameters were solved for as outputs.

To predict the impact of modulating an O_2 pathway parameter (eg, cardiac output) on $\dot{V}o_2$, the above procedure was run in reverse (Algorithm 2). The values of a patient's O_2 pathway parameters were specified as inputs and the patient's peak exercise responses, in particular, peak $\dot{V}o_2$, were solved for as outputs. Thus, an abnormal parameter such as cardiac output could be set to a normal reference value (Figure I in the online-only Data Supplement), and the expected improvement in a patient's peak $\dot{V}o_2$ could then be calculated (Algorithm 5). This boost in $\dot{V}o_2$ was normalized by expressing it as a fraction of the starting $\dot{V}o_2$ deficit (reference $\dot{V}o_2$ – measured $\dot{V}o_2$); the result was labeled the "$\dot{V}o_2$ deficit recovery" coefficient (VDR). Finally, a distinct metric of an O_2 pathway step's impact on $\dot{V}o_2$ was also calculated, the $\dot{V}o_2$ flux control coefficient.[18]

A very similar algorithm was used to quantify the impact of modulating multiple O_2 pathway parameters (Algorithm 6). When correcting multiple parameter defects, we distinguished between 2 related VDR calculations: (1) $\dot{V}o_2$ deficit recovery attributable to correcting multiple defects at once, eg, D_M, Q, and $\dot{V}_A$, denoted by $VDR_{D_M,Q,\dot{V}_A}$, and (2) $\dot{V}o_2$ deficit

recovery attributable to correcting 1 defect, eg, D_M, after first correcting a set of background defects, eg, Q and V_A, denoted by $VDR_{DM(Q,VA)}$. Detailed methods and all algorithms, including those used to create key figures, appear in the Methods in the online-only Data Supplement. Requests for data and analytic methods should be forwarded to the corresponding author.

Statistics

R was used for statistical analysis. Continuous measurements are presented as the mean±SEM unless otherwise stated. Distribution normality was assessed by using the Shapiro-Wilk test. Group characteristics were compared by using either the Student *t* test, the Kruskal-Wallis test, or the χ^2 test, as appropriate. A 2-sided *P* value<0.05 was considered statistically significant.

RESULTS

Patients with HFpEF (n=79) and controls (n=55) were of comparable age, sex, and body mass index (Table). Exercise capacity, defined as peak $\dot{V}o_2$, was reduced by 34±2% (*P*<0.001) in HFpEF relative to controls. We partitioned the O_2 pathway steps that explain this $\dot{V}o_2$ deficit into 2 categories, O_2 delivery and O_2 extraction, as detailed below.

Diagnosing O_2 Pathway Causes of Exercise Intolerance

O_2 Delivery

Total O_2 delivered to the periphery, defined as the product of cardiac output and arterial O_2 content at peak exercise, was reduced by 31±0.3% (*P*<0.001) in HFpEF compared with controls. This impairment was caused by a 27±3% (*P*<0.001) reduction in cardiac output and a 5±2% (*P*=0.02) reduction in hemoglobin concentration. Patients with HFpEF also harbored a 36±3% (*P*<0.001) reduction in alveolar ventilation and a 31±3% (*P*<0.001) reduction in lung diffusion capacity at peak exercise.

O_2 Extraction

Total O_2 extracted by the periphery, defined as the difference between arterial and venous O_2 content (ΔAVo_2) at peak exercise, was reduced by 8±2% (*P*=0.01) in HFpEF compared with controls. ΔAVo_2 has frequently been used as a metric of the periphery's ability to extract O_2[6,10,19–22] because it integrates the effects of multiple O_2 pathway steps. However, its value also depends on factors external to the periphery.[23] In particular, because of the competition between convective and diffusive transport of O_2, ΔAVo_2 depends on muscle blood flow and therefore cardiac output.

To evaluate the drawbacks of using ΔAVo_2 to gauge O_2 extraction by the periphery, we quantified the sensitivity of both ΔAVo_2 and $\dot{V}o_2$ to changes in cardiac output (Q) for a representative patient with HFpEF (Figure 2A, Algorithm 3). By explicitly accounting for the antagonism

Table. Baseline and Exercise Characteristics

Characteristic	Control (n=55)	HFpEF (n=79)	*P* Value
Anthropometrics			
Age, y	61 (11)	62 (11)	0.527
Sex: female	30 (55%)	35 (44%)	0.322
Weight, median (IQR), kg	83 (71–91)	87 (76–95)	0.097
Height, median (IQR), m	1.6 (1.6–1.7)	1.7 (1.6–1.8)	0.012
BMI, median (IQR), kg/m^2	29 (27–32)	30 (26–33)	0.687
Comorbidities			
Hypertension	29 (54%)	49 (62%)	0.437
Diabetes mellitus	3 (6%)	19 (24%)	0.010
Medications			
β-Blocker	17 (31%)	50 (64%)	<0.001
Calcium channel blocker	7 (13%)	12 (15%)	0.891
ACE inhibitor or ARB	15 (28%)	21 (27%)	1.000
Diuretic	10 (19%)	35 (44%)	0.004
Rest physiology			
LVEF, %	66 (6)	66 (7)	0.769
PAWP, median (IQR), mm Hg	11 (8–12)	16 (12–19)	<0.001
Hemoglobin, g/dL	14.1 (1.6)	13.4 (2.0)	0.015
eGFR, mL/min per 1.73 m^2	78 (17)	66 (22)	0.004
Peak exercise physiology			
Work, median (IQR), W	108 (86–173)	75 (54–94)	<0.001
$\dot{V}o_2$, median (IQR), L/min	1.62 (1.32–2.23)	1.09 (0.86–1.45)	<0.001
$\dot{V}o_2$, median (IQR), mL/min/kg	20 (16–27)	13 (11–16)	<0.001
% Predicted $\dot{V}o_2$, median (IQR)	103 (96–109)	66 (58–72)	<0.001
RER, median (IQR)	1.2 (1.1–1.2)	1.1 (1.1–1.2)	0.258
PAWP, median (IQR), mm Hg	22 (16–28)	26 (24–31)	0.001
Total ventilation, median (IQR), L/min	67 (55–93)	46 (36–63)	<0.001
$\dot{V}co_2$, median (IQR), L/min	1.94 (1.54–2.65)	1.26 (0.95–1.72)	<0.001
Alveolar ventilation, median (IQR), L/min	47 (39–67)	31 (24–45)	<0.001
Alveolar Po_2, mm Hg	120 (5)	119 (5)	0.051
Cardiac output, L/min	14.0 (3.6)	10.2 (3.1)	<0.001
Heart rate, beats/min	142 (18)	115 (25)	<0.001
Total O_2 delivery, median (IQR), L O_2/min	2.5 (2.0–3.4)	1.8 (1.4–2.2)	<0.001
ΔAVo_2, mL O_2 per dL blood	12.7 (2.3)	11.7 (2.2)	0.012

(*Continued*)

Table. Continued

Characteristic	Control (n=55)	HFpEF (n=79)	*P* Value
Arterial O_2 content, mL/dL	19 (2)	18 (3)	0.013
Arterial Po_2, median (IQR), mm Hg	97 (87–106)	96 (84–108)	0.980
Arterial O_2 saturation, median (IQR), %	100 (98–100)	99 (97–100)	0.057
Mixed venous O_2 content, mL/dL	6.5 (1.4)	6.5 (2.0)	0.796
Mixed venous Po_2, mm Hg	21 (2)	21 (3)	0.392
Mixed venous O_2 saturation, %	34 (7)	36 (9)	0.437
D_M, median (IQR), mL/min per mm Hg	48 (38–65)	32 (26–45)	<0.001
D_L, median (IQR), mL/min per mm Hg	22 (17–28)	15 (11–19)	<0.001

Table entries reflect mean (SD) or median (IQR) for continuous variables and n (%) for categorical variables. ACE indicates angiotensin-converting enzyme; ARB, angiotensin receptor blocker; BMI, body mass index (weight/height^2); ΔAVo_2, arteriovenous difference in oxygen content; D_L, pulmonary diffusion capacity for O_2; D_M, skeletal muscle diffusion capacity for O_2; eGFR, estimated glomerular filtration rate; HFpEF, heart failure with preserved ejection fraction; IQR, interquartile range; LVEF, left ventricular ejection fraction; Po_2, partial pressure of O_2; PAWP, pulmonary arterial wedge pressure; RER, respiratory exchange ratio; $\dot{V}co_2$, rate of carbon dioxide production; and $\dot{V}o_2$, rate of oxygen consumption.

between O_2 convection and diffusion, we found that doubling this patient's Q led to a 45% drop in ΔAVo_2. As a consequence, $\dot{V}o_2$ rose by only 10%. This is a notable departure from the doubling one might have predicted by simply applying the Fick equation, $\dot{V}o_2=Q\cdot\Delta AVo_2$.

We sought to enhance the interpretability of ΔAVo_2 as a metric of peripheral O_2 extraction by determining normal reference values for ΔAVo_2 when Q is impaired. Figure 2B displays the expected value of ΔAVo_2 at each value of Q for the control population (Algorithm 4). This locus of values serves as a calibration curve, indicating normal ΔAVo_2 at each possible value of Q. By comparing observed HFpEF ΔAVo_2 with the calibration curve value at observed HFpEF Q, we found that ΔAVo_2 was 26±2% (*P*<0.001) lower than predicted had O_2 extraction in HFpEF been normal (Figure 2B).

Using the ΔAVo_2 calibration curve, we went on to reinterpret ΔAVo_2 values reported in prior studies,[10,19–22] including those that had concluded that peripheral O_2 extraction in HFpEF was normal. We found that all 5 studies, each from a distinct laboratory, reported ΔAVo_2 values that fell short of normal ΔAVo_2 when controlled for Q (Figure 2C). We obtained similar results after repeating this analysis with ΔAVo_2 calibration curves derived from study-specific control populations (Figure II in the online-only Data Supplement). Thus controlling ΔAVo_2 for Q led to unanimous agreement between prior studies that O_2 extraction in HFpEF was impaired.

To identify the O_2 pathway step that impairs peripheral extraction in HFpEF, we calculated each patient's skeletal muscle diffusion capacity (D_M). Mean D_M was 36±2% (*P*<0.001) lower in patients with HFpEF than in controls (Figure 2D and 2E).

Impaired diffusion-mediated O_2 transport is a plausible mechanism of abnormal O_2 extraction in heart failure,[24] but impaired mitochondrial respiration could also contribute. We estimated that mitochondrial capacity for O_2 utilization (v_{max}) was reduced by 27±3% (*P*<0.001) in HFpEF relative to controls (Methods in the online-only Data Supplement). We conducted a sensitivity analysis to assess the degree to which our conclusions about D_M were influenced by our mitochondrial parameter estimates.[17] D_M in HFpEF remained impaired over virtually the entire range of mitochondrial parameters (Figure IIIA in the online-only Data Supplement).

Compound Mechanisms

After assessing each patient's full complement of O_2 pathway defects, we counted how often a defect occurred in isolation versus in concert with other defects. We termed the former "simple" mechanisms of exercise intolerance (Figure 3A) and the latter "compound" mechanisms. Strikingly, 97% of our patients with HFpEF harbored a compound mechanism (Figure 3B), with ≥2 defects in the O_2 pathway (<80% of the reference value).

Ranking O_2 Pathway Causes of Exercise Intolerance

We next used O_2 pathway analysis to gauge the functional significance of each of a patient's O_2 pathway defects. To rank defects by their causal impact on exercise capacity, we derived a novel property of the physiology, the VO2 deficit recovery (VDR) coefficient. The VDR coefficient for a given O_2 pathway defect is the normalized improvement in a patient's peak $\dot{V}o_2$ that would be expected from correcting the defect, while holding all other O_2 pathway parameters fixed.

We found that normalizing cardiac output would be predicted to improve the $\dot{V}o_2$ deficit in HFpEF by just 7±0.5% (mean VDR_Q=7%). VDR_Q could be estimated from the Fick equation alone ($\dot{V}o_2=Q\cdot\Delta AVo_2$), but this approach assumes that ΔAVo_2 would be unaffected by the rise in Q. When we calculated VDR_Q under this faulty assumption, the result overestimated deficit recovery by a factor of 10.

Of all the O_2 pathway defects in HFpEF, normalizing skeletal muscle diffusion capacity led to the largest predicted recovery of the $\dot{V}o_2$ deficit (Figure 4A). Mean VDR_{DM} was 27%, >3-fold higher than mean VDR_Q (*P*<0.001). As with estimates of D_M, VDR estimates are influenced by a patient's underlying mitochondrial function. In a sensitivity analysis, we found that the impact of D_M on exercise capacity exceeded that of Q over a wide range of mitochondrial respiration condi-

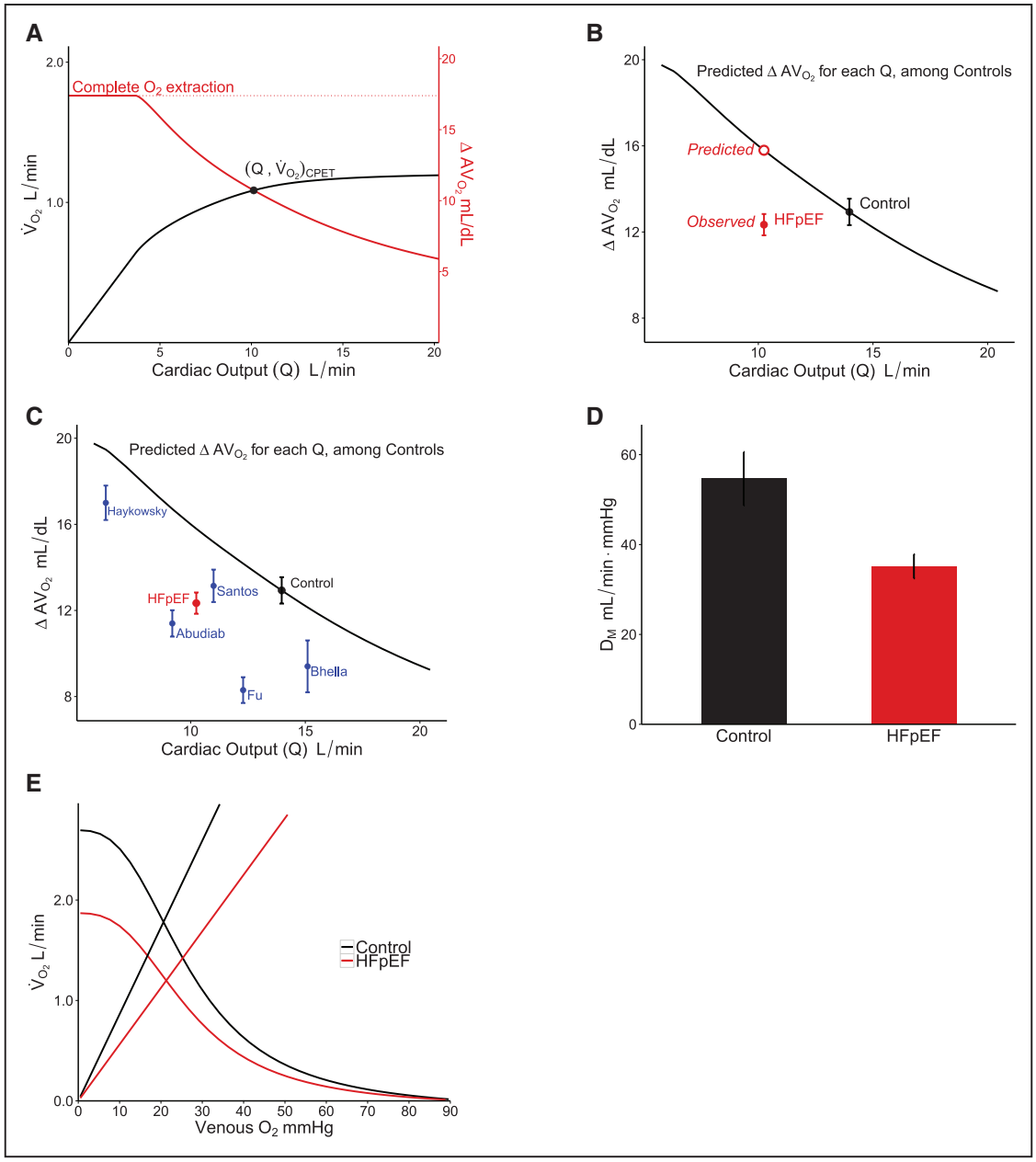

Figure 2. Peripheral oxygen extraction in HFpEF.

A, Antagonism between convective (cardiac) and diffusive delivery of O_2. The black point represents a typical patient with HFpEF from this study (median $\dot{V}o_2$), plotted at her CPET-derived values of peak exercise $\dot{V}o_2$, ΔAVo_2, and cardiac output (Q). The black and red curves display calculated values of this patient's $\dot{V}o_2$ and ΔAVo_2, respectively, over a range of Q values. "Complete O_2 extraction" indicates when the calculated venous Po_2 falls within 1 mm Hg of mitochondrial Po_2. **B**, Observed HFpEF ΔAVo_2 vs. control predicted ΔAVo_2. The red point represents mean ΔAVo_2 and Q in HFpEF. The black curve depicts the mean ΔAVo_2 vs. Q relationship in controls. The open circle denotes the predicted control value of ΔAVo_2 at the mean value of Q found in HFpEF. **C**, Published HFpEF ΔAVo_2 vs. control predicted ΔAVo_2. Mean ΔAVo_2 values from previously published HFpEF cohorts (blue points, annotated by first author) are plotted alongside the ΔAVo_2 vs. Q curve belonging to our control population. As in **B,** the red point denotes the mean HFpEF ΔAVo_2 measured in this study. All ΔAVo_2 values in **B** and **C** were scaled to the mean Hb level found in our controls. **D**, D_M in controls vs. HFpEF. **E**, Mean convective and diffusive components of O_2 transport in HFpEF vs. controls. The lines of O_2 convection (curved) depict $\dot{V}o_2$ as a function of venous Po_2 for fixed values of Q and arterial Po_2. The lines of O_2 diffusion (straight) depict $\dot{V}o_2$ as a function of venous Po_2 for fixed values of D_M and arterial Po_2. The intersection of these lines determines the $\dot{V}o_2$ achieved.[28] All error bars depict 95% confidence intervals. CPET indicates cardiopulmonary exercise testing; ΔAVo_2, arteriovenous difference in O_2 content; D_M, skeletal muscle diffusion capacity for O_2; Hb, hemoglobin concentration; HFpEF, heart failure with preserved ejection fraction; Po_2, partial pressure of O_2; and $\dot{V}o_2$, rate of O_2 consumption.

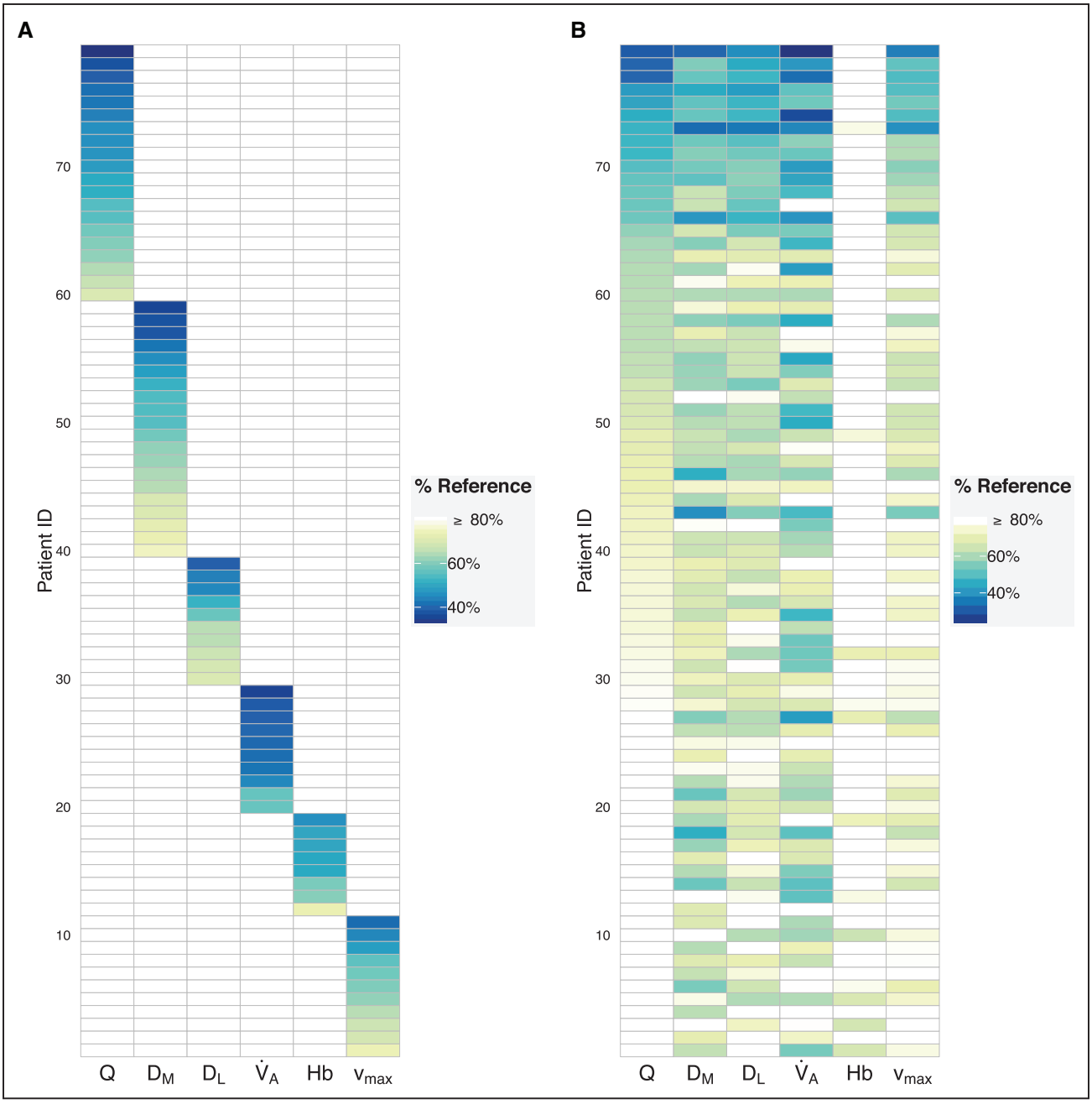

Figure 3. Simple vs. compound mechanisms of exercise intolerance.
A, Simulated patients with HFpEF (y axis), each with a single O_2 pathway defect. The x axis lays out each of the 6 distinct O_2 pathway parameters. The color of each tile indicates the severity of the defect, which is expressed as a percentage of the reference value (Figure II in the online-only Data Supplement). O_2 pathway parameters ≥80% of the reference value are considered normal and depicted as white tiles. Patients are sorted by the magnitude of their O_2 pathway defect. **B**, Patients with HFpEF from this study and their CPET-derived O_2 pathway defects. Patients are ordered by Q defect. CPET indicates cardiopulmonary exercise testing; D_L, lung diffusion capacity for O_2; D_M, skeletal muscle diffusion capacity for O_2; Hb, hemoglobin concentration; HFpEF, heart failure with preserved ejection fraction; Q, cardiac output; $\dot{V}_A$, alveolar ventilation; and v_{max}, mitochondrial respiration capacity.

tions (Figure IIIB in the online-only Data Supplement). Finally, we also compared the impact of D_M and Q on exercise capacity by using a distinct metric, the $\dot{V}o_2$ flux control coefficient. Its value for D_M was 2-fold higher than for Q ($P<0.001$; Figure IV in the online-only Data Supplement).

Context Dependence: The Influence of Comorbid Defects

We next examined factors that influence the magnitude of an O_2 pathway defect's impact on $\dot{V}o_2$. Because virtually all patients harbored multiple O_2 pathway defects,

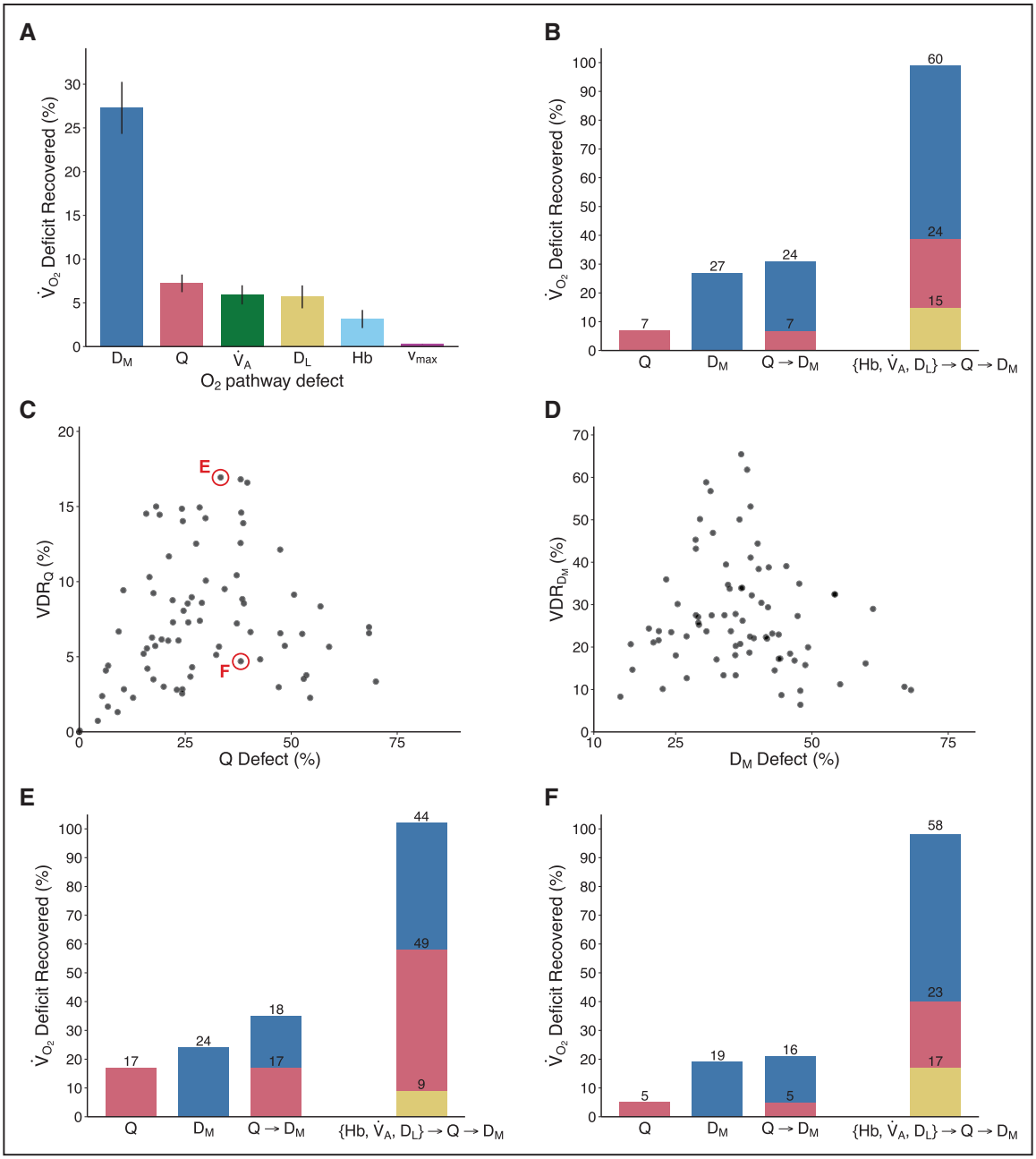

Figure 4. Causal influence of each O_2 pathway parameter on exercise capacity.
A, $\dot{V}o_2$ deficit recovery (VDR) coefficients for each O_2 pathway step in HFpEF. Error bars depict 95% confidence intervals. **B**, Influence of O_2 pathway background on VDR coefficients. The total height of each stack of bars reflects the VDR that results from correcting all associated parameters displayed under the stack. The height of each individual bar in the stack represents the VDR of 1 parameter after first correcting the parameters associated with the bars beneath it; this VDR value sits atop each bar. Bars are color coded to a unique parameter(s) (Q = red, D_M = blue, Hb + $\dot{V}_A$ + D_L = yellow). All VDR values reflect an average over all patients with HFpEF. **C**, VDR_Q vs. Q defect for each patient with HFpEF. Circled patients, E and F, are analyzed in **E** and **F**. **D**, VDR_{D_M} vs. D_M defect for each patient with HFpEF. In **C** and **D**, Q and D_M defects are expressed as 100% – ratio of the CPET-derived parameter to a reference value. **E** and **F**, Influence of O_2 pathway background on the VDR coefficients for 2 individual patients with a similar Q defect (circled in **C**). The meaning of these charts is identical to **B**, except that here each one characterizes an individual patient. CPET indicates cardiopulmonary exercise testing; D_L, lung diffusion capacity for O_2; D_M, skeletal muscle diffusion capacity for O_2; Hb, hemoglobin concentration; HFpEF, heart failure with preserved ejection fraction; and Q, cardiac output.

we investigated whether a given defect's VDR coefficient was influenced by a patient's comorbid O_2 pathway defects—the context. We calculated the impact of correcting D_M on a patient's $\dot{V}o_2$ under 3 conditions: (1) no change in background defects, denoted by VDR_{D_M} as above; (2) after first correcting Q, denoted $VDR_{D_M(Q)}$; and (3) after correcting Q together with O_2 pathway defects in the pulmonary ($\dot{V}_A$, D_L) and O_2-carrying steps

(Hb), denoted $VDR_{DM(Q,Hb,VA,DL)}$. Upon correction of multiple defects in the O_2 pathway background, we found that mean $VDR_{DM(Q,Hb,\ VA,DL)}$jumped to 60% of the initial $\dot{V}o_2$ deficit, >2-fold higher than VDR_{DM} (Figure 4B, bar 4, blue segment). Turning to the context dependence of VDR_Q, we found that first normalizing the O_2-loading system (Hb, V_A, D_L) subsequently tripled the impact of correcting Q, mean $VDR_{Q(Hb,VA,DL)}$=24% (Figure 4B, bar 4, red segment). These results demonstrate the dramatic role that background deficits could play in determining the efficacy of therapy.

After exploring the effects of context averaged over all patients with HFpEF, we examined its implications at the individual level. By plotting a patient's O_2 pathway defect versus its corresponding VDR coefficient, we discovered unanticipated heterogeneity among patients with the same-size defect (Figure 4C and 4D). For example, 2 patients with the same-size Q defect (Figure 4E and 4F) varied >3-fold in their predicted $\dot{V}o_2$ response to Q therapy (VDR_Q). Two patients with the same-size D_M defect exhibited VDR_{DM} values that varied as much as 7-fold.

Another surprising trend emerged from individual level data: the maximum VDR of an O_2 pathway defect diminished as the defect became more severe (Figure 4C and 4D). One might expect that correcting a severe defect would substantially benefit $\dot{V}o_2$. However, we found that individuals with 1 severe defect often harbored a high burden of comorbid O_2 pathway defects (Figure V in the online-only Data Supplement; Figure 3B). The VDR trend thus expresses the tyranny of comorbidities: as a patient's burden of O_2 pathway defects grows, the benefit of treating any one in isolation fades.

DISCUSSION

By reasoning about the pathophysiology of HFpEF from exercise data, we attempted to shed light on key clinical dilemmas in the field: How important is the periphery's contribution to exercise intolerance? How heterogeneous is HFpEF and why? What makes exercise intolerance so hard to treat? Answering these questions rested on 2 main tasks: diagnosing the causes of a patient's exercise intolerance and ranking their functional significance. First, we sought to deconstruct the pathophysiology of exercise intolerance by expressing it in terms of the component steps of O_2 transport and utilization (O_2 pathway). Cataloging each patient's O_2 pathway defects revealed a peripheral mechanism of disease previously uncharacterized in HFpEF, impaired skeletal muscle diffusion capacity. It also revealed extensive patient heterogeneity. HFpEF is classically regarded as a cardiac disorder, but we found that every O_2 pathway step was defective in 1 or more patients. What's more, this heterogeneity did not fit a tidy pattern of 1 defect per patient (Figure 3A). Most patients harbored a combination of defects (Figure 3B). The complex structure of this heterogeneity is at the heart of what makes exercise intolerance in HFpEF difficult to diagnose and treat. In the second phase of our analysis, we sought to quantify the impact of each O_2 pathway defect on a patient's exercise capacity. These properties of the physiology simultaneously inform personalized therapy (which defect has the largest impact?) and disease subtyping (which patients share a dominant defect?). To calculate these properties, we developed a novel tool, the VDR coefficient, which quantifies the causal impact of 1 O_2 pathway defect while accounting for the influence of comorbid defects. We found that even when a defect was large (eg, cardiac output), the predicted benefit of correcting it could be modest, because comorbid defects would hold $\dot{V}o_2$ recovery in check. The O_2 pathway step with the largest impact on exercise capacity was located in the periphery, skeletal muscle diffusion.

What limits exercise capacity in HFpEF? We chose to distill the mechanisms of disease down to elemental causes such as the O_2 pathway defects. Previous studies have associated HFpEF with pathologies such as left ventricular hypertrophy and vascular stiffness, or comorbidities such as aging, obesity, hypertension, and diabetes mellitus.[3] The mechanisms by which these factors influence exercise intolerance should be largely expressible in terms of O_2 pathway defects. Connecting the dots from upstream mechanisms to O_2 pathway defects will be an important direction of future research.

Here we reported the first systematic analysis of the O_2 pathway in HFpEF, but our findings for a subset of O_2 pathway steps are corroborated by prior studies. For example, similar reductions in $\dot{V}o_2$ and cardiac output at peak exercise have been widely reported in HFpEF.[10,21] Abnormalities of skeletal muscle[25] and pulmonary function,[26] including a comparable reduction in peak lung diffusion capacity,[12] have also been reported, although relatively underappreciated. Recently, the contribution of peripheral O_2 extraction, as measured by ΔAVo_2, to exercise intolerance has received greater attention. However, despite close interstudy agreement regarding the absolute value of ΔAVo_2 in HFpEF (when measured invasively, Figure 2C),[6,10,21] the role of the periphery remains unsettled.

The Periphery's Contribution to Exercise Intolerance

Opinions regarding the causal significance of the periphery in HFpEF are divided, but they can be reconciled by analyzing O_2 extraction in terms of its component O_2 pathway steps. At the heart of the discord lies an insidious misconception, that the periphery's ability to extract O_2 can be gauged by the total O_2 actually ex-

tracted (ΔAVo_2). Using ΔAVo_2 as a metric of O_2 extraction, studies that reported similar values in HFpEF and controls concluded that peripheral abnormalities cannot explain exercise intolerance.[10,21] Studies that reported a reduction in HFpEF ΔAVo_2 relative to controls concluded that the periphery cannot be ignored.[6,19,20] To resolve this dilemma, we first note that a conventional cardiopulmonary exercise testing analysis leans heavily on the Fick equation to dissect exercise capacity: $\dot{V}o_2 = Q \cdot \Delta AVo_2$. This equation invites the mistaken impression that cardiac output (Q) and ΔAVo_2 are independent of each other. Although ΔAVo_2 integrates the effects of multiple noncardiac O_2 pathway steps, its value depends on the heart as well: the faster an O_2-carrying red blood cell races through a capillary, the less time O_2 has to diffuse into muscle mitochondria, which leaves more O_2 unextracted and, in turn, raises venous O_2 content. Consequently, if at peak exercise Q were to rise further—all else being equal—ΔAVo_2 would fall due to decreased time available for diffusion.[27,28] Conversely, if Q were to fall, ΔAVo_2 would rise (Figure 2A). Confusion in the field has arisen because ΔAVo_2 in isolation has been used to gauge the performance of the periphery, overlooking its dependence on Q. To untangle the two, we had to explicitly account for the O_2 pathway steps that drive peripheral extraction, including diffusion and mitochondrial respiration, together with their relationship to Q. By unpacking the ΔAVo_2 term in this way, we showed that when prior studies were reinterpreted to account for impaired Q, they all reported ΔAVo_2 values in HFpEF that were inappropriately low (Figure 2C). O_2 pathway analysis thus unifies the evidence that the peripheral response to exercise in HFpEF is impaired.

What causes impaired peripheral extraction? We identified impaired skeletal muscle diffusion capacity as a novel defect in HFpEF. O_2 moves from the muscle microcirculation to the mitochondria by diffusion. This process depends on both muscle capillarity and muscle fiber size, which together determine the diffusion capacity for O_2.[29] Our data cannot identify the specific pathology that accounts for reduced diffusion capacity, but the work of others has shown that capillary to fiber ratios are reduced in HFpEF.[25]

Patient Heterogeneity

Is HFpEF one disease or many?[30,31] If it is many diseases, then this heterogeneity could itself span a spectrum of complexity. At one extreme, HFpEF could be a structured set of 1-problem disorders (simple mechanisms), wherein each patient harbors a single defect in the O_2 pathway. Such patients would fall neatly into disease subtypes, one for each O_2 pathway step (Figure 3A). At the opposite extreme, HFpEF could be a loose collection of multiproblem disorders. Indeed, we found that nearly every patient harbored a compound mechanism of exercise intolerance, each with his or her own personal profile of defects (Figure 3B). In addition to muddying the taxonomy of HFpEF, compound mechanisms raise hard questions about treatment: When a patient's exercise intolerance has multiple causes, how significant is each one's contribution to symptoms?

Clinical Implications

To address questions germane to therapy and diagnosis, we shifted our focus from quantifying the O_2 pathway defects to quantifying their causal impact on exercise capacity. We cast the problem of personalizing therapy as deciding which of a patient's O_2 pathway defects has the largest causal impact and thus the greatest therapeutic potential. We found that the magnitude of a defect's impact on $\dot{V}o_2$ depended not only on the defect itself but also on a patient's entire array of comorbid defects. In a patient with 1 lone defect (simple mechanism), the magnitude of its causal impact on $\dot{V}o_2$ can be stated trivially: it accounts for 100% of the $\dot{V}o_2$ deficit. But in HFpEF, our data suggest that simple mechanisms are the exception and compound mechanisms the rule. When multiple O_2 pathway defects coexist, quantifying causal effects is no longer straightforward. Defects interact. From the viewpoint of the heart, these interactions may drastically alter the relationship between cardiac output and exercise capacity. Consequently, the magnitude of cardiac output's impact on $\dot{V}o_2$ is a system property—it depends on all comorbid O_2 pathway defects and cannot be judged by the size of the cardiac output defect alone. Accounting for comorbid defects, we showed that in HFpEF, the predicted impact of normalizing cardiac output on the $\dot{V}o_2$ deficit is modest, an average improvement of 7%. The notion that comorbidities herald a difficult disease course is familiar to clinicians of all stripes. For exercise intolerance in HFpEF, O_2 pathway analysis shows how this notion can be granted causal, quantitative precision.

Why are patients with HFpEF so hard to treat? The system properties of their exercise pathophysiology offer a compelling explanation: the benefit of correcting any single O_2 pathway defect would be reined in by comorbid defects. Cardiac output is particularly susceptible to such interactions, because its augmentation comes at the cost of diffusive O_2 transport in both the lungs and skeletal muscle. These processes are impaired in HFpEF[12] (Table) and may help explain why cardiocentric therapies have not been successful to date. Current and future trials of cardiac output therapies, eg, rate-adaptive atrial pacing, will further test these concepts. Exercise end points such as peak $\dot{V}o_2$ and actigraphy metrics[32] would be particularly valuable in such trials, because cardiac end points in isolation could paint an incomplete picture of therapeutic efficacy. In contrast, peak $\dot{V}o_2$ integrates the entire O_2 pathway, explaining its potent prognostic value in heart failure.

The system properties of the O_2 pathway clarify another key observation in HFpEF, the efficacy of exercise training.[33] Exercise training is capable of boosting multiple O_2 pathway steps, including skeletal muscle diffusion capacity,[34] lung diffusion capacity,[35] mitochondrial respiration capacity,[36] and cardiac output[37]; in HFpEF, specifically, these effects have been shown to manifest as enhanced ΔAVo_2.[22,38] Thus, even though the benefits of exercise on symptoms may not come as a great surprise, O_2 pathway analysis provides a causal, quantitative basis for its unique salutary effects.

The same analysis we used to inform the personalization of therapy, diagnosing and ranking O_2 pathway defects, can also be applied to disease subtyping. Heterogeneity within our HFpEF cohort reflects each patient's individual profile of O_2 pathway defects. Because a central aim of diagnosis is to link symptoms to their cause, this heterogeneity presents a challenge for HFpEF nosology. One solution would be to first characterize a patient's O_2 pathway defects through exercise testing and then assign him or her to a subgroup of patients with shared defects, eg, "HFpEF-Q". Such a diagnostic label would answer the question: What's abnormal (Figure 5A)? The relevance of this scheme to therapy may be limited, however, because 2 individuals could have the same Q defect, but radically different responses to Q therapy (Figure 4E and 4F). Caution is therefore warranted if patients are to be grouped together by virtue of a common O_2 pathway defect, a seemingly natural criterion for defining a subtype of disease or for including patients in a clinical trial. Perhaps a HFpEF taxonomy should group patients with shared susceptibilities to therapy. The diagnostic label could then reflect shared causal impact of an O_2 pathway defect, HFpEF-VDR_Q, answering the question: What should we treat (Figure 5B)? The VDR coefficients are patient-centric measures of a defect's causal impact and thus natural metrics by which to gauge patient similarity for disease subtyping.

To estimate a patient's O_2 pathway defects and their functional impact, we used exercise testing with invasive monitoring. Although not routine clinical practice, this approach is increasingly common and, in some cases, guideline-recommended to aid in the diagnosis of HFpEF.[39] Advances in noninvasive techniques for measuring cardiac output, blood gas levels,[40] and skeletal muscle properties could facilitate the widespread use of O_2 pathway analysis. This study highlights the rationale and unmet need for such a systematic analysis of a patient's pathophysiology—in particular, the role of the periphery.

Study Limitations

Our patients with HFpEF were selected from a referral population and differed from clinical trial populations[41–43]

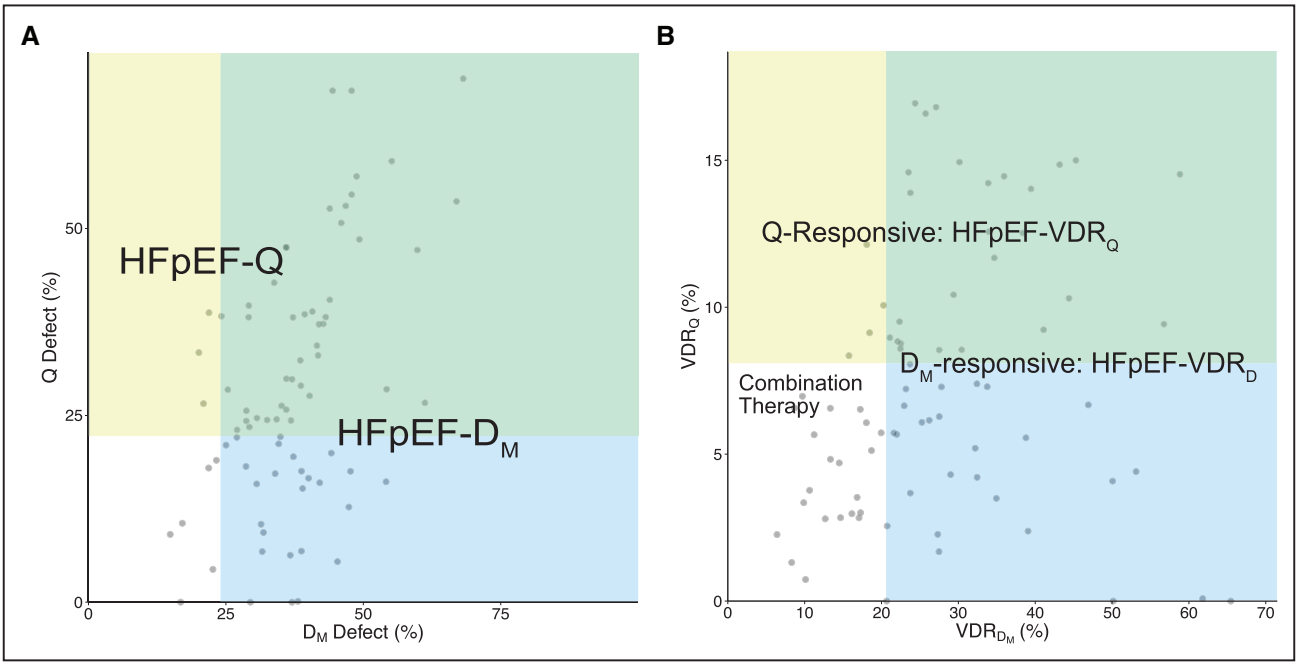

Figure 5. Subtyping HFpEF by exercise pathophysiology.
A, Scatter plot of patients with HFpEF by O_2 pathway defects, Q vs. D_M. Illustrative taxonomy of HFpEF based on shared O_2 pathway defects. **B**, Scatter plot of patients with HFpEF by VDR coefficients (VDR_Q vs. VDR_{D_M}). Illustrative taxonomy of HFpEF based on shared susceptibility to O_2 pathway therapy (Q vs. D_M therapy). "Combination therapy" represents a subgroup of patients for whom a meaningful increase in $\dot{V}o_2$ would require correcting multiple O_2 pathway parameters. D_M indicates skeletal muscle diffusion capacity for O_2; HFpEF, heart failure with preserved ejection fraction; Q, cardiac output; and VDR, $\dot{V}o_2$ deficit recovery.

in several respects. They were younger, were more predominantly male, and exhibited lower rates of diabetes mellitus and hypertension. When we recalculated key results in patients >60 years of age and stratified by sex, we observed similar Q and D_M defects and similar values of VDR_Q and VDR_{DM} (Table II in the online-only Data Supplement). However, a strength of our study was the use of characteristic symptoms together with invasive hemodynamic measurements when defining HFpEF. Furthermore, our patients did share important similarities with trial populations, including comparable peak $\dot{V}o_2$ and hemodynamic measurements (Table), echocardiographic parameters (66% with left atrial enlargement), and heart failure hospitalization rates (18% per year).

Peak volitional effort is critical to implicating O_2 pathway steps as causes of exercise intolerance. To maximize the likelihood that peak effort was achieved, we excluded patients in whom respiratory exchange ratio did not reach 1.0, and we noted that peak respiratory exchange ratio was nearly identical between HFpEF and controls (mean respiratory exchange ratio of 1.16 versus 1.17 in HFpEF versus controls and interquartile range, 1.1–1.2 in both groups).

We used mixed venous O_2 levels to estimate muscle diffusion capacity. Although the majority of venous return emerges from the femoral veins during cycle ergometry, more refined estimates of D_M could be made with local (femoral) measurements of blood flow and O_2 levels (Methods in the online-only Data Supplement). Furthermore, the degree of mismatch between blood flow and metabolism within muscle will also be important to determine.[44,45]

To estimate the impact of manipulating an O_2 pathway defect, we based our analysis on the causal physical principles that underlie the physiology. One limitation of our approach is that we did not account for possible biological adaptations, namely that modulating 1 O_2 pathway step could, over time, trigger changes in other steps. That said, all our $\dot{V}o_2$ predictions were explicitly conditioned on holding those remaining O_2 pathway parameters fixed. Future intervention studies, accompanied by pre- and postintervention O_2 pathway analysis, could reveal the existence and magnitude of such biological adaptations.

Conclusions

Overcoming the treatment impasse in HFpEF hinges on an improved understanding of disease pathophysiology. Exercise intolerance is a heterogeneous, difficult-to-treat symptom, because a typical patient harbors a compound mechanism of disease, with a unique profile of O_2 pathway defects, each of which exerts a context-sensitive and rarely dominant influence on exercise capacity. Personalized measures of causal influence such as the VDR coefficients could be used to stratify patients for clinical trials and for diagnostic purposes to tailor therapy. Finally, the system properties of the physiology favor therapies that influence multiple O_2 pathway steps simultaneously, in particular, exercise training.

ACKNOWLEDGMENTS

We would like to thank K. Bakken, C. White, and G. Cotter (Massachusetts General Hospital) for clinical support. We would also like to thank M. Giannakis (Dana Farber Institute), A. Philippakis (Broad Institute), N. Chatterjee (Massachusetts General Hospital), and A. Bellinger (Brigham and Women's Hospital) for their critical review of the manuscript, and S. Aiello (WordsWorld) for editorial support.

SOURCES OF FUNDING

This work was supported by grants from the John S. LaDue Foundation and the Margaret Q. Landenberger Foundation (to Dr Houstis) and American Heart Association Awards 15GPSGC24800006 and NHLBI R01-HL131029 (to Dr Lewis).

DISCLOSURES

None.

AFFILIATIONS

Cardiology Division, Department of Medicine, Massachusetts General Hospital, Boston (N.E.H., A.S.E., P.P.P., L.W., C.S.B., G.D.L.). School of Medicine, University of California, San Diego (P.D.W.).

FOOTNOTES

Received April 20, 2017; accepted September 19, 2017.

The online-only Data Supplement is available with this article at http://circ.ahajournals.org/lookup/suppl/doi:10.1161/CIRCULATIONAHA.117.029058/-/DC1.

Continuing medical education (CME) credit is available for this article. Go to http://cme.ahajournals.org to take the quiz.

Circulation is available at http://circ.ahajournals.org.

REFERENCES

1. Zile MR, Baicu CF, Gaasch WH. Diastolic heart failure–abnormalities in active relaxation and passive stiffness of the left ventricle. *N Engl J Med*. 2004;350:1953–1959. doi: 10.1056/NEJMoa032566.
2. Houstis NE, Lewis GD. Causes of exercise intolerance in heart failure with preserved ejection fraction: searching for consensus. *J Card Fail*. 2014;20:762–778. doi: 10.1016/j.cardfail.2014.07.010.
3. Bench T, Burkhoff D, O'Connell JB, Costanzo MR, Abraham WT, St John Sutton M, Maurer MS. Heart failure with normal ejection fraction: consideration of mechanisms other than diastolic dysfunction. *Curr Heart Fail Rep*. 2009;6:57–64.
4. Burkhoff D, Maurer MS, Packer M. Heart failure with a normal ejection fraction: is it really a disorder of diastolic function? *Circulation*. 2003;107:656–658.
5. Upadhya B, Haykowsky MJ, Eggebeen J, Kitzman DW. Exercise intolerance in heart failure with preserved ejection fraction: more than a heart

problem. *J Geriatr Cardiol*. 2015;12:294–304. doi: 10.11909/j.issn.1671-5411.2015.03.013.
6. Dhakal BP, Malhotra R, Murphy RM, Pappagianopoulos PP, Baggish AL, Weiner RB, Houstis NE, Eisman AS, Hough SS, Lewis GD. Mechanisms of exercise intolerance in heart failure with preserved ejection fraction: the role of abnormal peripheral oxygen extraction. *Circ Heart Fail*. 2015;8:286–294. doi: 10.1161/CIRCHEARTFAILURE.114.001825.
7. Shah SJ, Kitzman DW, Borlaug BA, van Heerebeek L, Zile MR, Kass DA, Paulus WJ. Phenotype-specific treatment of heart failure with preserved ejection fraction: a multiorgan roadmap. *Circulation*. 2016;134:73–90. doi: 10.1161/CIRCULATIONAHA.116.021884.
8. Wasserman K. *Principles of Exercise Testing and Interpretation: Including Pathophysiology and Clinical Applications*. 5th ed. Philadelphia, PA: Wolters Kluwer Health/Lippincott Williams & Wilkins; 2012.
9. Weibel ER. *The Pathway for Oxygen: Structure and Function in the Mammalian Respiratory System*. Cambridge, MA: Harvard University Press; 1984.
10. Abudiab MM, Redfield MM, Melenovsky V, Olson TP, Kass DA, Johnson BD, Borlaug BA. Cardiac output response to exercise in relation to metabolic demand in heart failure with preserved ejection fraction. *Eur J Heart Fail*. 2013;15:776–785. doi: 10.1093/eurjhf/hft026.
11. Molina AJ, Bharadwaj MS, Van Horn C, Nicklas BJ, Lyles MF, Eggebeen J, Haykowsky MJ, Brubaker PH, Kitzman DW. Skeletal muscle mitochondrial content, oxidative capacity, and Mfn2 expression are reduced in older patients with heart failure and preserved ejection fraction and are related to exercise intolerance. *JACC Heart Fail*. 2016;4:636–645. doi: 10.1016/j.jchf.2016.03.011.
12. Olson TP, Johnson BD, Borlaug BA. Impaired pulmonary diffusion in heart failure with preserved ejection fraction. *JACC Heart Fail*. 2016;4:490–498. doi: 10.1016/j.jchf.2016.03.001.
13. Shafiq A, Brawner CA, Aldred HA, Lewis B, Williams CT, Tita C, Schairer JR, Ehrman JK, Velez M, Selektor Y, Lanfear DE, Keteyian SJ. Prognostic value of cardiopulmonary exercise testing in heart failure with preserved ejection fraction. The Henry Ford HospITal CardioPulmonary EXercise Testing (FIT-CPX) project. *Am Heart J*. 2016;174:167–172. doi: 10.1016/j.ahj.2015.12.020.
14. Jones NL. *Clinical Exercise Testing*. 3rd ed. Philadelphia, PA: Saunders; 1988.
15. Vasan RS, Levy D. Defining diastolic heart failure: a call for standardized diagnostic criteria. *Circulation*. 2000;101:2118–2121.
16. Borlaug BA, Jaber WA, Ommen SR, Lam CS, Redfield MM, Nishimura RA. Diastolic relaxation and compliance reserve during dynamic exercise in heart failure with preserved ejection fraction. *Heart*. 2011;97:964–969. doi: 10.1136/hrt.2010.212787.
17. Cano I, Mickael M, Gomez-Cabrero D, Tegnér J, Roca J, Wagner PD. Importance of mitochondrial P(O2) in maximal O2 transport and utilization: a theoretical analysis. *Respir Physiol Neurobiol*. 2013;189:477–483. doi: 10.1016/j.resp.2013.08.020.
18. Fell D. *Understanding the Control of Metabolism*. 1st ed. London, UK: Portland Press; 1997.
19. Bhella PS, Prasad A, Heinicke K, Hastings JL, Arbab-Zadeh A, Adams-Huet B, Pacini EL, Shibata S, Palmer MD, Newcomer BR, Levine BD. Abnormal haemodynamic response to exercise in heart failure with preserved ejection fraction. *Eur J Heart Fail*. 2011;13:1296–1304. doi: 10.1093/eurjhf/hfr133.
20. Haykowsky MJ, Brubaker PH, John JM, Stewart KP, Morgan TM, Kitzman DW. Determinants of exercise intolerance in elderly heart failure patients with preserved ejection fraction. *J Am Coll Cardiol*. 2011;58:265–274. doi: 10.1016/j.jacc.2011.02.055.
21. Santos M, Opotowsky AR, Shah AM, Tracy J, Waxman AB, Systrom DM. Central cardiac limit to aerobic capacity in patients with exertional pulmonary venous hypertension: implications for heart failure with preserved ejection fraction. *Circ Heart Fail*. 2015;8:278–285. doi: 10.1161/CIRCHEARTFAILURE.114.001551.
22. Fu TC, Yang NI, Wang CH, Cherng WJ, Chou SL, Pan TL, Wang JS. Aerobic interval training elicits different hemodynamic adaptations between heart failure patients with preserved and reduced ejection fraction. *Am J Phys Med Rehabil*. 2016;95:15–27. doi: 10.1097/PHM.0000000000000312.
23. Wagner PD. A theoretical analysis of factors determining VO2 MAX at sea level and altitude. *Respir Physiol*. 1996;106:329–343.
24. Esposito F, Mathieu-Costello O, Shabetai R, Wagner PD, Richardson RS. Limited maximal exercise capacity in patients with chronic heart failure: partitioning the contributors. *J Am Coll Cardiol*. 2010;55:1945–1954. doi: 10.1016/j.jacc.2009.11.086.
25. Kitzman DW, Nicklas B, Kraus WE, Lyles MF, Eggebeen J, Morgan TM, Haykowsky M. Skeletal muscle abnormalities and exercise intolerance in older patients with heart failure and preserved ejection fraction. *Am J Physiol Heart Circ Physiol*. 2014;306:H1364–H1370. doi: 10.1152/ajpheart.00004.2014.
26. Andrea R, López-Giraldo A, Falces C, Sobradillo P, Sanchis L, Gistau C, Heras M, Sabate M, Brugada J, Agustí A. Lung function abnormalities are highly frequent in patients with heart failure and preserved ejection fraction. *Heart Lung Circ*. 2014;23:273–279. doi: 10.1016/j.hlc.2013.08.003.
27. Piiper J, Scheid P. Modeling oxygen availability to exercising muscle. *Respir Physiol*. 1999;118:95–101.
28. Wagner PD. Modeling O_2 transport as an integrated system limiting (.) V(O_2MAX). *Comput Methods Programs Biomed*. 2011;101:109–114. doi: 10.1016/j.cmpb.2010.03.013.
29. Wagner PD. Diffusive resistance to O2 transport in muscle. *Acta Physiol Scand*. 2000;168:609–614. doi: 10.1046/j.1365-201x.2000.00712.x.
30. Borlaug BA. Is HFpEF one disease or many? *J Am Coll Cardiol*. 2016;67:671–673. doi: 10.1016/j.jacc.2015.11.045.
31. Kosmala W, Rojek A, Przewlocka-Kosmala M, Mysiak A, Karolko B, Marwick TH. Contributions of nondiastolic factors to exercise intolerance in heart failure with preserved ejection fraction. *J Am Coll Cardiol*. 2016;67:659–670. doi: 10.1016/j.jacc.2015.10.096.
32. Redfield MM, Anstrom KJ, Levine JA, Koepp GA, Borlaug BA, Chen HH, LeWinter MM, Joseph SM, Shah SJ, Semigran MJ, Felker GM, Cole RT, Reeves GR, Tedford RJ, Tang WH, McNulty SE, Velazquez EJ, Shah MR, Braunwald E; NHLBI Heart Failure Clinical Research Network. Isosorbide mononitrate in heart failure with preserved ejection fraction. *N Engl J Med*. 2015;373:2314–2324. doi: 10.1056/NEJMoa1510774.
33. Kitzman DW, Brubaker P, Morgan T, Haykowsky M, Hundley G, Kraus WE, Eggebeen J, Nicklas BJ. Effect of caloric restriction or aerobic exercise training on peak oxygen consumption and quality of life in obese older patients with heart failure with preserved ejection fraction: a randomized clinical trial. *JAMA*. 2016;315:36–46. doi: 10.1001/jama.2015.17346.
34. Boushel R, Ara I, Gnaiger E, Helge JW, González-Alonso J, Munck-Andersen T, Sondergaard H, Damsgaard R, van Hall G, Saltin B, Calbet JA. Low-intensity training increases peak arm VO2 by enhancing both convective and diffusive O2 delivery. *Acta Physiol (Oxf)*. 2014;211:122–134. doi: 10.1111/apha.12258.
35. Guazzi M, Reina G, Tumminello G, Guazzi MD. Improvement of alveolar-capillary membrane diffusing capacity with exercise training in chronic heart failure. *J Appl Physiol (1985)*. 2004;97:1866–1873. doi: 10.1152/japplphysiol.00365.2004.
36. Hambrecht R, Fiehn E, Yu J, Niebauer J, Weigl C, Hilbrich L, Adams V, Riede U, Schuler G. Effects of endurance training on mitochondrial ultrastructure and fiber type distribution in skeletal muscle of patients with stable chronic heart failure. *J Am Coll Cardiol*. 1997;29:1067–1073.
37. Stratton JR, Levy WC, Cerqueira MD, Schwartz RS, Abrass IB. Cardiovascular responses to exercise. Effects of aging and exercise training in healthy men. *Circulation*. 1994;89:1648–1655.
38. Haykowsky MJ, Brubaker PH, Stewart KP, Morgan TM, Eggebeen J, Kitzman DW. Effect of endurance training on the determinants of peak exercise oxygen consumption in elderly patients with stable compensated heart failure and preserved ejection fraction. *J Am Coll Cardiol*. 2012;60:120–128. doi: 10.1016/j.jacc.2012.02.055.
39. Ponikowski P, Voors AA, Anker SD, Bueno H, Cleland JG, Coats AJ, Falk V, González-Juanatey JR, Harjola VP, Jankowska EA, Jessup M, Linde C, Nihoyannopoulos P, Parissis JT, Pieske B, Riley JP, Rosano GM, Ruilope LM, Ruschitzka F, Rutten FH, van der Meer P; Authors/Task Force Members. 2016 ESC Guidelines for the diagnosis and treatment of acute and chronic heart failure: The Task Force for the diagnosis and treatment of acute and chronic heart failure of the European Society of Cardiology (ESC). Developed with the special contribution of the Heart Failure Association (HFA) of the ESC. *Eur Heart J*. 2016;37:2129–2200. doi: 10.1093/eurheartj/ehw128.
40. Mathewson KW, Haykowsky MJ, Thompson RB. Feasibility and reproducibility of measurement of whole muscle blood flow, oxygen extraction, and VO2 with dynamic exercise using MRI. *Magn Reson Med*. 2015;74:1640–1651. doi: 10.1002/mrm.25564.
41. Redfield MM, Chen HH, Borlaug BA, Semigran MJ, Lee KL, Lewis G, LeWinter MM, Rouleau JL, Bull DA, Mann DL, Deswal A, Stevenson LW, Givertz MM, Ofili EO, O'Connor CM, Felker GM, Goldsmith SR, Bart BA, McNulty SE, Ibarra JC, Lin G, Oh JK, Patel MR, Kim RJ, Tracy RP, Velazquez EJ, Anstrom KJ, Hernandez AF, Mascette AM, Braunwald E; RELAX Trial. Effect of phosphodiesterase-5 inhibition on exercise capac-

ity and clinical status in heart failure with preserved ejection fraction: a randomized clinical trial. *JAMA*. 2013;309:1268–1277. doi: 10.1001/jama.2013.2024.
42. Massie BM, Carson PE, McMurray JJ, Komajda M, McKelvie R, Zile MR, Anderson S, Donovan M, Iverson E, Staiger C, Ptaszynska A; I-PRESERVE Investigators. Irbesartan in patients with heart failure and preserved ejection fraction. *N Engl J Med*. 2008;359:2456–2467. doi: 10.1056/NEJMoa0805450.
43. Cleland JG, Tendera M, Adamus J, Freemantle N, Polonski L, Taylor J; PEP-CHF Investigators. The perindopril in elderly people with chronic heart failure (PEP-CHF) study. *Eur Heart J*. 2006;27:2338–2345. doi: 10.1093/eurheartj/ehl250.
44. Heinonen I, Koga S, Kalliokoski KK, Musch TI, Poole DC. Heterogeneity of muscle blood flow and metabolism: influence of exercise, aging, and disease states. *Exerc Sport Sci Rev*. 2015;43:117–124. doi: 10.1249/JES.0000000000000044.
45. Louvaris Z, Habazettl H, Asimakos A, Wagner H, Zakynthinos S, Wagner PD, Vogiatzis I. Heterogeneity of blood flow and metabolism during exercise in patients with chronic obstructive pulmonary disease. *Respir Physiol Neurobiol*. 2017;237:42–50. doi: 10.1016/j.resp.2016.12.013.

Exercise Intolerance in Heart Failure With Preserved Ejection Fraction: Diagnosing and Ranking Its Causes Using Personalized O2 Pathway Analysis

Nicholas E. Houstis, Aaron S. Eisman, Paul P. Pappagianopoulos, Luke Wooster, Cole S. Bailey, Peter D. Wagner and Gregory D. Lewis

Circulation. 2018;137:148-161; originally published online October 9, 2017;
doi: 10.1161/CIRCULATIONAHA.117.029058
Circulation is published by the American Heart Association, 7272 Greenville Avenue, Dallas, TX 75231

Print ISSN: 0009-7322. Online ISSN: 1524-4539

Supplemental Material

Supplemental Material

Table of Contents:

1. Supplemental Methods

1.1 Exercise Testing

After placement of pulmonary and radial artery catheters patients performed a maximum incremental upright cycle ergometry CPET (5-25 Watts/min continuous ramp after an initial 3-minute period of unloaded exercise, MedGraphics, St. Paul, MN) with simultaneous hemodynamic monitoring (Witt Biomedical Inc, Melbourne, FL), as previously described.[1] None of the subjects developed angina, arrhythmia, hypotension or significant electrocardiographic changes during exercise. We measured right atrial pressure, mean pulmonary arterial pressure, pulmonary arterial wedge pressure (PAWP), and systemic arterial pressures at end-expiration, in multiple positions and time points: at rest while supine or seated upright on the cycle, and during exercise with sequential measurements at one-minute intervals. Peak $\dot{V}_{O_2}$was defined as the highest O_2 uptake, averaged over 30 seconds, during the last minute of symptom-limited exercise. First-pass radionuclide ventriculography of both ventricles was performed immediately before cycle ergometry.

An exercise test that ends prematurely could confound the identification of impaired O_2 pathway steps. We therefore designed this study to employ upright exercise that would maximize exercise performance and only evaluated exercise tests in which a patient's RER exceeded 1.0. The achievement of nearly identical average peak RER values of 1.16 and 1.17 in HFpEF and controls, along with marked increases in lactate levels, and peak workloads in excess of those reported in other HFpEF studies,[2] suggests that premature exercise cessation was not common among HFpEF patients in this study. We did not observe an association between peak PAWP and peak cardiac output (ρ=-0.02, p=0.87) or between peak PAWP and peak $\dot{V}_{O_2}$(ρ=0.1, p=0.37) among HFpEF patients, consistent with previous studies in HFrEF.[3] These observations are evidence that patients did not stop exercising prematurely on account of PAWP elevation.

1.2 Exercise Physiology Model and Core Algorithms for Parameter Estimation

The equations governing O_2 transport and utilization described below link the physiology of four systems[4-8]: pulmonary, cardiac, blood, and skeletal muscle. Together these systems deliver O_2 from inspired air to the respiring mitochondria of skeletal muscle. They are coupled together in series (the O_2 pathway), such that any individual system influences O_2 handling in all the rest. The integrated nature of the system as a

whole implies that to predict the influence of one step, e.g. cardiac output, on an output such as peak $\dot{V}_{O_2}$, one must account for as many of the other steps as possible.

The system of equations we used to quantify O_2 transport and utilization appear below (Eqs. 1-2, 6-11, Table S1). None of the equations are novel; they have been used individually for decades. Equations 1 and 2 describe diffusive transport in the pulmonary and skeletal muscle capillaries respectively. The appearance of cardiac output (Q) in these equations accounts for the antagonism between convection and diffusion that plays such a central role in our analysis. Equation 7 describes the Fick principle, which relates $\dot{V}_{O_2}$, cardiac output, and blood O_2 concentrations based on the law of O_2 mass conservation. This Fick equation is one of the most widely used equations in clinical cardiology. Equation 8 relates $\dot{V}_{O_2}$ to mitochondrial pO_2 based on hyperbolic Michaelis-Menten-like kinetics, a relationship with considerable experimental support.[9] Equation 9 is an approximation to maximal mitochondrial respiration that we derived based on prior studies in humans (see details below). Equations 10 and 11 describe pulmonary gas exchange using mass balance relationships that are also heavily used in clinical practice. Each of the biophysical principles described by these equations was discovered many years ago and has been extensively validated. Our goal here was to work out their implications as an interconnected whole for exercise physiology in HFpEF.

Table S1. Notation

Q	Cardiac Output (L min^{-1})
$\dot{V}_{O_2}$	Oxygen consumption (mL min^{-1})
$\dot{V}_{CO_2}$	Carbon dioxide production (mL min^{-1})
$\dot{V}_A$	Alveolar ventilation (mL min^{-1})
$P_{I_{O_2}}$	Inspired partial pressure of oxygen (mmHg)
k	Units conversion constant = 1.159 (mL O_2 mL^{-1} air mmHg^{-1})
Pa_{O_2}	Arterial partial pressure of oxygen (mmHg)
$P\bar{v}_{O_2}$	Mixed venous partial pressure of oxygen (mmHg)
Pa_{CO_2}	Arterial partial pressure of carbon dioxide (mmHg)
Hb	Hemoglobin concentration (mg dL^{-1} blood)
ΔAV_{O_2}	Arterio-venous oxygen content difference (mL O_2 dL^{-1} blood)
P_{mito}	Intramitochondrial partial pressure of oxygen (mmHg)
p_{50}	Mitochondrial oxygen affinity (mmHg)
v_{max}	Total oxidative phospohorylation capacity (mL O_2 min^{-1})
D_M	Skeletal muscle diffusion capacity for oxygen (mL O_2 min^{-1} mmHg^{-1})

$P_{A_{O_2}}$	Alveolar partial pressure of oxygen (mmHg)
D_L	Pulmonary diffusion capacity for oxygen (mL O_2 min^{-1} $mmHg^{-1}$)
$P_{Lcap}(t)$	O_2 concentration in the pulmonary capillaries, as a function of time (mmHg)
$P_{Mcap}(t)$	O_2 concentration in the skeletal muscle capillaries, as a function of time (mmHg)
T	Capillary transit time (min)
$c_{O_2}(x, Hb)$	O_2 Content Function:[10] Total O_2 concentration of the blood (mL O_2 L^{-1} blood), as a function of dissolved O_2 concentration (mmHg), x, and Hemoglobin concentration (mg dL^{-1}), Hb

In the first half of our analysis we estimated each patient's O_2 pathway parameters at peak exercise. These parameters are the equation constants that quantify each step of O_2 transport and utilization, including alveolar ventilation ($\dot{V}_A$), the pulmonary diffusion capacity of O_2 (D_L), cardiac output (Q), the skeletal muscle diffusion capacity (D_M), and the maximum respiration capacity of mitochondria (v_{max}). Hemoglobin levels were directly measured. The mitochondrial p_{50} of O_2 respiration was set at a reference value (see below). The governing equations can be solved for these parameters by plugging in measurements from a patient's cardiopulmonary exercise test. These include $\dot{V}_{O_2}, \dot{V}_{CO_2}, Pa_{CO_2}, Pa_{O_2}, P\bar{v}_{O_2}, Hb$. The whole procedure is described in pseudocode as Algorithm 1.

In the second half of our analysis our goal was to predict the impact on $\dot{V}_{O_2}$ of changing an O_2 pathway parameter. This is conceptually analogous to the common practice of using the Fick equation alone for such predictions. For example, in a patient with low cardiac output, it would be tempting to conclude that $\dot{V}_{O_2}$ would rise proportionally with Q correction, in accordance with Fick: $\dot{V}_{O_2} = Q \cdot \Delta AV_{O_2}$. The critical flaw in this logic is that ΔAV_{O_2} will also change upon Q correction (it will fall), with the potential to seriously undermine the benefit of Q augmentation, as detailed in the main text. To improve on $\dot{V}_{O_2}$ predictions, the remedy is to use the entire system of equations rather than Fick in isolation. We accomplish this by using the same equations (expressed slightly differently) as in Algorithm 1, but with the inputs and outputs reversed. In Algorithm 2 we plug O_2 pathway parameter values (e.g. high Q) in to the equations and solve for the system's quantitative responses, e.g. $\dot{V}_{O_2}$.

The paradigm outlined above also generalizes to predicting the impact on $\dot{V}_{O_2}$ of changing *multiple* O_2 pathway parameters. Another example is helpful here: if a patient's cardiac output were low, and they were anemic, one might be inclined to predict the result of treating these conditions on $\dot{V}_{O_2}$ by plugging normal values of cardiac output and hemoglobin in to the Fick equation. As in the one parameter case

above, rather than use Fick in isolation, we consider the entire system's response to these changes. The estimated impact on $\dot{V}_{O_2}$ with this approach often differs significantly from Fick-based predictions. The details appear in Algorithm 6.

Throughout this work we focused on the physiology of peak exercise. All of the measurements we used and all O_2 pathway parameters we calculated were in the state of peak exercise. To streamline this exposition, we often omit the modifier "at peak exercise", except on occasion for emphasis.

We implemented all algorithms and performed all data analyses in the R programming language. We used the R package bvpSolve to solve the governing equations.

O_2 Transport Equations, Lung (L) and Muscle (M):

$$\frac{dP_{Lcap}(t)}{dt} = \frac{D_L}{QTc'_{O_2}\left(P_{Lcap}(t), Hb\right)}\left(P_{A_{O_2}} - P_{Lcap}(t)\right) \quad (1)$$

$$\frac{dP_{Mcap}(t)}{dt} = -\frac{D_M}{QTc'_{O_2}\left(P_{Mcap}(t), Hb\right)}\left(P_{Mcap}(t) - P_{mito}\right) \quad (2)$$

Boundary Conditions, Algorithm 1:

$$P_{Mcap}(0) = Pa_{O_2} \quad (3)$$

$$P_{Lcap}(0) = P\bar{v}_{O_2} \quad (4)$$

$$P_{Mcap}(T) = P\bar{v}_{O_2} \quad (5)$$

$$P_{Lcap}(T) = Pa_{O_2} \quad (6)$$

Algebraic Constraints, Algorithm 1:

$$Q = \frac{\dot{V}_{O_2}}{\left(c_{O_2}(Pa_{O_2}, Hb) - c_{O_2}\left(P\bar{v}_{O_2}, Hb\right)\right)} \quad (7)$$

$$P_{mito} = \frac{p_{50}}{\frac{v_{max}}{\dot{V}_{O_2}} - 1} \quad (8)$$

$$v_{max} = R_{mito}\dot{V}_{O_2} \quad (9)$$

$$P_{A_{O_2}} = P_{I_{O_2}} - \frac{\dot{V}_{O_2}}{\dot{V}_A k} \quad (10)$$

$$\dot{V}_A = \frac{\dot{V}_{CO_2}}{kPa_{CO_2}} \quad (11)$$

Algorithm 1: O_2 pathway parameter estimation from an individual's exercise measurements

1. Input:
   a) CPET-measurements at peak exercise for patient i: $\dot{V}_{O_2}, \dot{V}_{CO_2}, Pa_{CO_2}, Pa_{O_2}, P\bar{v}_{O_2}, Hb$
   b) Constants: $k, P_{I_{O_2}}, p_{50}, R_{mito}^{Ctl}, R_{mito}^{HF}$
2. Solve O_2 transport equations (1)-(2), (7)-(11) with boundary conditions (3)-(6)
3. Output:
   a) Patient i's O_2 pathway parameters at peak exercise: $Q, D_L, D_M, \dot{V}_A, v_{max}$
   b) Patient i's O_2 tension in the alveolus, mitochondria, pulmonary and muscle capillaries: $P_{A_{O_2}}, P_{mito}, P_{Lcap}(t), P_{Mcap}(t)$

Boundary Conditions and Constraints, Algorithm 2:

$$P_{Lcap}(0) = P_{Mcap}(T) \quad (12)$$

$$P_{Lcap}(T) = P_{Mcap}(0) \quad (13)$$

$$\dot{V}_{O_2} = Q\left(c_{O_2}\left(P_{Mcap}(0), Hb\right) - c_{O_2}\left(P_{Mcap}(T), Hb\right)\right) \quad (14)$$

$$P_{mito} = \frac{p_{50}}{\frac{v_{max}}{\dot{V}_{O_2}} - 1} \quad (15)$$

$$P_{A_{O_2}} = P_{I_{O_2}} - \frac{\dot{V}_{O_2}}{\dot{V}_A k} \quad (16)$$

Algorithm 2: Calculate a patient's O_2 levels from their O_2 pathway parameters

1. Input:
   a) O_2 pathway parameters at peak exercise for patient i: $Q, D_L, D_M, \dot{V}_A, p_{50}, v_{max}, Hb$
   b) Constants: $P_{I_{O_2}}$

   Input values could either have been estimated using Algorithm 1, measured directly (e.g. Hb), or deliberately set in order to study the properties of patient i's physiology.

2. Solve O_2 transport equations (1)-(2), (14)-(16) with boundary conditions (12)-(13)

3. Output:
   a) O_2 levels at peak exercise: $\dot{V}_{O_2}, \Delta AV_{O_2}, P_{Lcap}(t), P_{Mcap}(t), Pa_{O_2}, P\bar{v}_{O_2}, P_{mito}, P_{A_{O_2}}$

In the above formulation of the transport and utilization equations we model the entire periphery as a single muscle compartment. This approach was necessitated by the fact that our venous blood samples were drawn from the pulmonary artery rather than femoral vein. Such practice is consistent with virtually all previously published work in HFpEF. One limitation of the single compartment approach is that high venous O_2 levels could be mistakenly attributed to impaired skeletal muscle extraction when in fact the cause was shunting of blood flow away from the leg muscles, or even microvascular shunting (flow/respiration mismatch). If there were a systematic difference between HFpEF and controls with respect to either form of shunting (not assessed in this study), it could have influenced our estimates of skeletal muscle diffusion capacity and the relative difference between groups. There are two lines of evidence to suggest that large vessel shunting of blood is unlikely in HFpEF. First, Esposito et al[11] performed femoral venous sampling and femoral blood flow measurements, during exercise, in heart failure with reduced ejection fraction (HFrEF) patients as well as controls. They showed that the fraction of cardiac output directed to the femoral arteries, at peak exercise, was in fact equivalent between between HFrEF and controls (68% vs 64% respectively). The pathophysiology of HFrEF likely shares features with HFpEF and arguably provides at least a bound on the severity of shunting. A second line of evidence, in this case from HFpEF patients, Hundley et al[12] measured flow mediated dilation of the superficial femoral arteries and found no significant difference between HFpEF and controls. Another consequence of the single compartment model is that the estimated value of D_M will reflect the diffusing capacity of two exercising legs. As defined here, D_M is an extensive property, with a value that depends on the total mass of exercising muscle and total O_2 delivery. Consequently, the value of D_M for two exercising legs reported here, will be larger than the value estimated from measurements of a single leg.[11]

To model the blood compartment, we used measured hemoglobin values together with the oxygen dissociation curve of Dash and Bassingthwaighte.[10]

To incorporate mitochondrial respiration in to our analysis, we expressed it as a function of intramitochondrial O_2 tension, P_{mito}.[5, 9] The in vivo measurement of P_{mito} at peak exercise is very demanding[13] and to our knowledge has not been reported in heart failure patients. In lieu of measuring P_{mito}, we estimated it from a patient's $\dot{V}_{O_2}$, together with two kinetic parameters that characterize the O_2 dependence of the mitochondrial respiration curve, p_{50} and v_{max}(eqns. 8 and 15).[5, 9] These kinetic parameters are themselves difficult to measure in vivo and in particular at peak exercise. However, values of p_{50} and v_{max} have been previously reported, including from both health and disease settings. We used these reference values in our calculations as described below.

We used a single reference value of p_{50}, the effective O_2 affinity of mitochondrial respiration, for both HFpEF and controls in all main text calculations. This value, $p_{50} = 0.24$mmHg, was previously derived from ex vivo measurements of isolated fibroblasts from healthy individuals in state 3 respiration.[14] To determine the influence of this choice on our conclusions we performed a sensitivity analysis. In Figure S3 we reassessed our key findings over a range of pathologic (i.e. high) values of p_{50} with an upper bound of 0.74mmHg. This pathologic value was measured in cells from individuals with Leigh syndrome,[14] a grave mitochondrial disorder with impaired cytochrome oxidase function that is typically fatal at a young age.

We derived individualized estimates of mitochondrial v_{max} using a patient's measured $\mathrm{peak}\,\dot{V}_{O_2}$, together with reference values of "reserve mitochondrial capacity" as defined below. v_{max} quantifies the maximum rate of oxygen consumption that can be supported by the sum of all exercising muscle mitochondria. Since the overwhelming majority of O_2 is consumed by mitochondria at peak exercise, $\mathrm{peak}\,\dot{V}_{O_2}$ should not exceed v_{max}. Indeed, studies suggest that v_{max} exceeds $\mathrm{peak}\,\dot{V}_{O_2}$ by a factor as high as 2.0 during bipedal exercise. We refer to the ratio $v_{max}/\mathrm{peak}\,\dot{V}_{O_2}$ as an individual's "reserve mitochondrial respiration capacity", R_{mito}. With this definition, we can estimate an individual's v_{max} by measuring their $\mathrm{peak}\,\dot{V}_{O_2}$ and multiplying it by an appropriate reference value of R_{mito}.

Esposito et al[11] were the first to assess the relationship between v_{max} and $\mathrm{peak}\,\dot{V}_{O_2}$ in patients with HFrEF in vivo, laying the foundation for our approach. Without directly measuring v_{max} they showed that it exceeds $\mathrm{peak}\,\dot{V}_{O_2}$ in both HFrEF and controls. Using their published data, we estimated lower bounds on the reserve mitochondrial capacity, R_{mito}, in HFrEF and controls. Our motivation for deriving a lower bound is that as R_{mito} increases its influence on our conclusions rapidly diminishes, as large values imply that

mitochondrial respiration capacity is present in excess (see sensitivity analysis in section 2.4). We were thus interested in the smallest value of R_{mito} supported by data.

To explain the logic behind our lower bound on R_{mito}, we briefly review Esposito et al's experimental design.[11] In what follows all references to blood flow and $\dot{V}_{O_2}$ occur in the context of peak exercise, so for brevity we drop the modifier "peak". Esposito measured blood flow and $\dot{V}_{O_2}$ in a single leg (femoral blood sampling) under two exercise conditions, single-leg knee extension (KE) and bipedal cycling. They deliberately chose this comparison since *blood flow* to a leg performing 1-leg knee extensions is higher than it is to a leg performing bipedal cycling, *per kilogram of exercising muscle*. In other words, simply by changing exercise modality the investigators could increase the rate of convective O_2 delivery to the exercising leg, per mass of exercising muscle. If a patient harbored reserve mitochondrial respiratory capacity during bipedal exercise, ie, $R_{mito} = v_{max}^{(\mathrm{Cycle})}/\dot{V}_{O_2}^{(\mathrm{Cycle})} > 1$, then with augmented O_2 delivery that patient could tap in to their mitochondrial reserve and raise O_2 consumption per unit muscle: $\dot{V}_{O_2}^{(\mathrm{KE})}/M_{\mathrm{KE}} > \dot{V}_{O_2}^{(\mathrm{Cycle})}/M_{\mathrm{Cycle}}$ (where $\dot{V}_{O_2}$ is O_2 consumption by the single leg being measured and M denotes the mass of exercising muscle in that leg). Conversely, in the absence of mitochondrial reserve ie, $v_{max}^{(\mathrm{Cycle})} \approx \dot{V}_{O_2}^{(\mathrm{Cycle})}$, augmenting O_2 delivery by switching to single-leg knee extension would be powerless to raise O_2 consumption per unit muscle, since mitochondria could support no additional respiration. An absence of reserve would thus imply: $\dot{V}_{O_2}^{(\mathrm{KE})}/M_{\mathrm{KE}} \approx \dot{V}_{O_2}^{(\mathrm{Cycle})}/M_{\mathrm{Cycle}}$. What Esposito et al[11] in fact observed was that $\dot{V}_{O_2}^{(\mathrm{KE})}/M_{\mathrm{KE}}$ was roughly twice as great as $\dot{V}_{O_2}^{(\mathrm{Cycle})}/M_{\mathrm{Cycle}}$ in both HFrEF and controls, reflecting significant reserve capacity for mitochondrial respiration during bipedal exercise. Their data on the ratio $\frac{\dot{V}_{O_2}^{(\mathrm{KE})}/M_{\mathrm{KE}}}{\dot{V}_{O_2}^{(\mathrm{Cycle})}/M_{\mathrm{Cycle}}}$ enabled us to establish a lower bound for R_{mito}, the quantity we wish to estimate. Consider HFrEF, where they found this ratio equaled 2.0:

$$\frac{\dot{V}_{O_2}^{(\mathrm{KE})}}{M_{\mathrm{KE}}} \leq \frac{v_{max}^{(\mathrm{KE})}}{M_{\mathrm{KE}}} \quad (17)$$

$$\frac{\dot{V}_{O_2}^{(\mathrm{KE})}/M_{\mathrm{KE}}}{\dot{V}_{O_2}^{(\mathrm{Cycle})}/M_{\mathrm{Cycle}}} = 2.0 \quad (18)$$

$$\frac{v_{max}^{(\mathrm{Cycle})}}{M_{\mathrm{Cycle}}} = \frac{v_{max}^{(\mathrm{KE})}}{M_{\mathrm{KE}}} \geq \frac{\dot{V}_{O_2}^{(\mathrm{KE})}}{M_{\mathrm{KE}}} = 2.0 * \frac{\dot{V}_{O_2}^{(\mathrm{Cycle})}}{M_{\mathrm{Cycle}}} \quad (19)$$

$$R_{mito}^{HFrEF} \equiv \frac{v_{max}^{(\mathrm{Cycle})}}{\dot{V}_{O_2}^{(\mathrm{Cycle})}} \geq 2.0 \quad (20)$$

Equation 17 expresses a constraint of the physiology, that O_2 consumption during exercise is bounded by the maximum capacity for O_2 respiration in mitochondria. Equation 18 is derived from measurements reported in Esposito et al for HFrEF.[11] Equation 19 combines equations 17, 18, and the observation that v_{max}/M is an approximately intensive (i.e. size-invariant) property of muscle. This bound on R_{mito} has the attractive property that it is derived from data collected *in vivo*, at peak exercise. Furthermore, our estimate of R_{mito} derived from control patients in Esposito et al[11] is 1.8, remarkably close to the value of 1.6 reported by Boushel et al[15] in healthy individuals using a completely different method. The latter study compared ex vivo oxidative phosphorylation capacity in isolated skeletal muscle mitochondria (giving an estimate of v_{max}) to in vivo $\mathrm{peak}\,\dot{V}_{O_2}$. Finally, Mettauer et al[16] measured v_{max} ex vivo in HFrEF and found that it was equivalent to controls, despite a significant reduction in peak $\dot{V}_{O_2}$in HFrEF. Their findings reinforce the notion that R_{mito} is at least as large in HFrEF as it is in controls.

In summary, we calculated individualized estimates of v_{max} for each of our study participants using bounds on R_{mito} that we derived from data reported in Esposito et al[11]: $R_{mito}^{HFrEF} \geq 2.0$ and $R_{mito}^{Control} \geq 1.8$. In particular, for each control patient we set $v_{max} = 1.8 \cdot \mathrm{peak}\,\dot{V}_{O_2}$, and for each heart failure patient we set $v_{max} = 2.0 \cdot \mathrm{peak}\,\dot{V}_{O_2}$. As with our choice of p_{50}, we performed a sensitivity analysis to assess the impact of these R_{mito} values on our key findings (Figure S3).

1.3 Algorithms for key Figure calculations

Below we provide pseudocode for four algorithms used to generate key Figures.

Algorithm 3 describes the calculations we used to generate Figure 2a. This figure displays $\dot{V}_{O_2}$ and ΔAV_{O_2} as a function of cardiac output.

Algorithm 3: Figure 2a. Elucidate the dependence of ΔAV_{O_2} and $\dot{V}_{O_2}$ on cardiac output (Q) in HFpEF

1. Select an individual whose physiology can illustrate this relationship: choose the patient with median $\dot{V}_{O_2}$ in the HFpEF study population.
2. Use Algorithm 1 to determine this patient's O_2 pathway parameters from their CPET measurements.
3. Specify a range of Q-values over which to study the interaction between $\dot{V}_{O_2}$, ΔAV_{O_2} and Q. For each Q_{new} in this range:
   i. Fix all O_2 pathway parameters except Q at their values calculated in step 2.
   ii. Use Algorithm 2 to calculate ΔAV_{O_2} and $\dot{V}_{O_2}$ at Q_{new}.

It's worth noting that the observed relationship, the increase in peripheral O_2 extraction as cardiac output falls, reflects intrinsic physical properties of the O_2 transport and utilization system. It does not reflect (nor account for) any adaptive biological response to changes in Q.

Algorithm 4 describes the calculations we used to generate Figure 2b. Our goal was to perform a controlled comparison of ΔAV_{O_2} between two groups whose cardiac outputs differ. In particular, we used these calculations to determine whether ΔAV_{O_2} in HFpEF is impaired relative to controls, while controlling for the fact that Q is reduced in HFpEF.

Algorithm 4: Figure 2b. Gauge peripheral O_2 extraction in HFpEF using a calibration curve of ΔAV_{O_2} values derived from Controls

1. Calculate the mean value of each O_2 pathway parameter, averaging over the control patients (Algorithm 1). Define a new patient with "mean control physiology" to have O_2 pathway parameters equal to the control population averages.
2. Specify a range of Q-values for which a normal value of $\Delta \mathrm{AV}_{\mathrm{O}_2}$ is desired. For each Q_{new} in this range:
   i. For the "mean control patient" defined in step 1, fix all O_2 parameters except Q.
   ii. Use Algorithm 2 to calculate the value of ΔAV_{O_2} at Q_{new}.
   iii. Plot $(Q_{new}, \Delta AV_{O_2})$
3. To implicate a peripheral extraction defect in HFpEF:
   i. Adjust for anemia: If Control Hb > HFpEF Hb, scale HFpEF ΔAV_{O_2} by a factor equal to the ratio of Control Hb to HFpEF Hb
   ii. Plot the observed group average of $(Q, \Delta AV_{O_2})$ in HFpEF
   iii. Compare the observed HFpEF ΔAV_{O_2} with the ΔAV_{O_2} value predicted by the calibration curve, at the observed HFpEF value of Q. By construction, this curve's ΔAV_{O_2} values reflect normal peripheral extraction at each possible value of Q. Extraction is impaired if the observed HFpEF ΔAV_{O_2} is smaller than the calibration curve prediction.

Algorithm 5 describes the calculations we used to compute the $\dot{V}_{O_2}$ deficit recovery coefficient (VDR) for a given O_2 pathway parameter in an individual patient. In brief, we calculated the improvement in the patient's peak $\dot{V}_{O_2}$ expected from correcting one parameter defect, while holding the remaining O_2 pathway parameters constant. In effect, we gauged a defect's causal impact by "subtracting" it. We expressed the $\dot{V}_{O_2}$ boost as a fraction of the starting $\dot{V}_{O_2}$ deficit (reference $\dot{V}_{O_2}$ – measured $\dot{V}_{O_2}$) and called this metric the "$\dot{V}_{O_2}$ deficit recovery" coefficient (VDR).

For concreteness, we describe the calculation of VDR_Q but the calculations would be identical for any O_2 pathway parameter with one exception. To identify the reference value for hemoglobin we used standard clinical reference values.

Algorithm 5: Figure 4a. VDR_Q calculation for an individual patient

1. Determine the reference value of cardiac output, Q_{ref}, for patient i. This reference value reflects normal peak cardiac output, adjusted for age, height, and gender.
   i. Construct a linear model of Q as a function of peak $\dot{V}_{O_2}$, using CPET-data from this study's *control* population. See Supplemental Figure 1 where this regression is plotted.
   ii. Calculate patient i's predicted peak $\dot{V}_{O_2}$ using an established formula[17] that adjusts for height, age, and gender:
   $$\dot{V}_{O_2} = 0.83 * Height^{2.7}(1 - 0.007 * Age)(1 - 0.2 * Female)$$
   iii. Estimate patient i's Q_{ref} as the value of Q predicted by the linear model from step i, at the peak predicted $\dot{V}_{O_2}$ determined in step ii. In essence, we determine Q_{ref} by answering the question: What would Q have been if the patient's peak $\dot{V}_{O_2}$ were normal?
2. Fix all O_2 parameters at patient i's CPET-derived values (Algorithm 1), except for Q.
   i. If $Q_{CPET} < Q_{ref}$, set $Q = Q_{ref}$.
   ii. If $Q_{CPET} \geq Q_{ref}$, then patient i's cardiac output is normal, and there is no Q-defect to correct. Therefore $VDR_Q = 0$.
3. Using Algorithm 2, calculate the predicted value of $\dot{V}_{O_2}$ at Q_{ref}: call it the "boosted" $\dot{V}_{O_2}$.
4. Define the $\dot{V}_{O_2}$ deficit recovery coefficient for Q ie, VDR_Q, to be the fraction of the patient's $\dot{V}_{O_2}$ deficit that would be recovered by boosting Q to Q_{ref}:

$$VDR_Q = \frac{\text{boosted } \dot{V}_{O_2} - \text{ observed } \dot{V}_{O_2}}{\text{peak predicted } \dot{V}_{O_2} - \text{ observed } \dot{V}_{O_2}}$$

Note that although each O_2 pathway defect accounts for a fraction of a patient's $\dot{V}_{O_2}$deficit, the sum of the VDR coefficients may actually exceed 100%. This occurs, on occasion, when one or more of a patient's *unaffected* O_2 pathway parameters actually exceed their reference values. Consequently, when all defects are corrected, the final boosted $\dot{V}_{O_2}$will exceed the predicted $\dot{V}_{O_2}$ due to the presence of supra-normal O_2 pathway parameters.

Algorithm 6 describes the calculations we used to plot Figure 4b. It is a minor extension of Algorithm 5 wherein we calculate the VDR due to correcting *multiple* O_2 pathway parameters rather than a single parameter. We distinguish between two such VDR calculations. In the first case, we calculate the $\dot{V}_{O_2}$deficit recovery due to correcting an entire subset of defects at once (e.g. defects X,Y,Z) and denote the coefficient: $VDR_{X,Y,Z}$. In the second case, we are interested in the $\dot{V}_{O_2}$deficit recovery due to X *after* first correcting Y and Z, which we denote as $VDR_{X(Y,Z)}$. The purpose of this latter calculation is to compare the causal impact of X on different "backgrounds" of O_2 pathway defects, eg, $VDR_{X(Y,Z)}$ vs VDR_X.

Algorithm 6: Figure 4b. VDR calculations for a set of O_2 pathway parameters

1. Determine the reference values of $Q, D_L, D_M, \dot{V}_A, Hb, v_{max}$ for patient i.
   i. For parameters $Q, D_L, D_M, \dot{V}_A$, identify their reference values using the linear models described in Algorithm 5 and displayed in Supplemental Figure 1.
   ii. For Hb, use the reference value 13.5 mg/dL for women and 15 mg/dL for men, or patient i's Hb, whichever is higher.
   iii. For v_{max}, the reference value is $1.8 * \text{peak predicted } \dot{V}_{O_2}$ (see mitochondrial discussion in section 1.2), where patient i's $\text{peak predicted } \dot{V}_{O_2}$ is calculated as in Algorithm 5.
2. Correct the desired subset of background O_2 parameters: assign them patient i's reference values, with the remainder assigned i's CPET-derived values (Algorithm 1).
3. Use Algorithm 2 to calculate the boosted $\dot{V}_{O_2}$ at the values of the O_2 parameters assigned in step 2. Calculate the VDR coefficient as in Algorithm 5.

$VDR_{X,Y}$ vs $VDR_{X(Y)}$ eg, $X = D_M, Y = Q$:

i. $VDR_{D_M,Q}$: *Total* height of Bar 3 in Figure 4b: set both Q and D_M to their reference values and calculate the $\text{boosted } \dot{V}_{O_2}$ and then the VDR:

$$VDR_{D_M,Q} = \frac{D_M \text{ and } Q \text{ boosted } \dot{V}_{O_2} - \text{ observed } \dot{V}_{O_2}}{\text{peak predicted } \dot{V}_{O_2} - \text{ observed } \dot{V}_{O_2}}$$

ii. $VDR_{D_M(Q)}$: height of the D_M component of Bar 3 in Figure 4b: the height of this bar reflects *sequential* parameter correction.

$$VDR_{D_M(Q)} = \frac{D_M \text{ and } Q \text{ boosted } \dot{V}_{O_2} - Q \text{ boosted } \dot{V}_{O_2}}{\text{peak predicted } \dot{V}_{O_2} - \text{ observed } \dot{V}_{O_2}}$$

$$= \frac{D_M \text{ and } Q \text{ boosted } \dot{V}_{O_2} - \text{ observed } \dot{V}_{O_2}}{\text{peak predicted } \dot{V}_{O_2} - \text{ observed } \dot{V}_{O_2}} - \frac{Q \text{ boosted } \dot{V}_{O_2} - \text{ observed } \dot{V}_{O_2}}{\text{peak predicted } \dot{V}_{O_2} - \text{ observed } \dot{V}_{O_2}}$$

$$= VDR_{D_M,Q} - VDR_Q$$

$\dot{V}_{O_2}$ recovery is always measured relative to a fixed denominator representing the observed $\dot{V}_{O_2}$ deficit.

2. Supplemental Data

2.1 Results stratified by age and gender

To assess the impact of patient demographics on our findings, we recalculated key results in a subset of older study participants, stratified by gender. The results appear in Table S2 below.

HFpEF Characteristics	ALL HFpEF	Females>60yo	Males>60yo
Age	62 (11)	69 (6)	72 (8)
BMI	30 (5)	30 (4)	28 (4)
Peak $\dot{\mathbf{V}}_{\mathbf{O_2}}$ (% predicted)	64 (11)	67 (6)	61 (12)
Q Defect (100 - % predicted)	28 (17)	23 (11)	35 (19)
D_M Defect (100 - % predicted)	37 (11)	34 (9)	39 (12)
VDR_Q (%)	7.2 (4)	7.6 (5)	7.1 (5)
VDR_{DM} (%)	27 (13)	29 (10)	22 (10)

2.2 Reference values of O_2 pathway parameters

To predict the impact of normalizing an O_2 pathway parameter on exercise capacity, we required normal ("reference") values of these parameters. For several of these parameters, normal values can be expected to depend on gender, age, and body size. A convenient way to capture these dependencies is via their relationship to peak $\dot{V}_{O_2}$, which has similar dependencies. Below we determined the empirical relationship of key O_2 pathway parameters to $\dot{V}_{O_2}$ in our control population (at peak exercise), individuals whose peak $\dot{V}_{O_2}$ is very near their age-, gender-, and height- predicted values (mean percent predicted $\dot{V}_{O_2}$ = 104%).

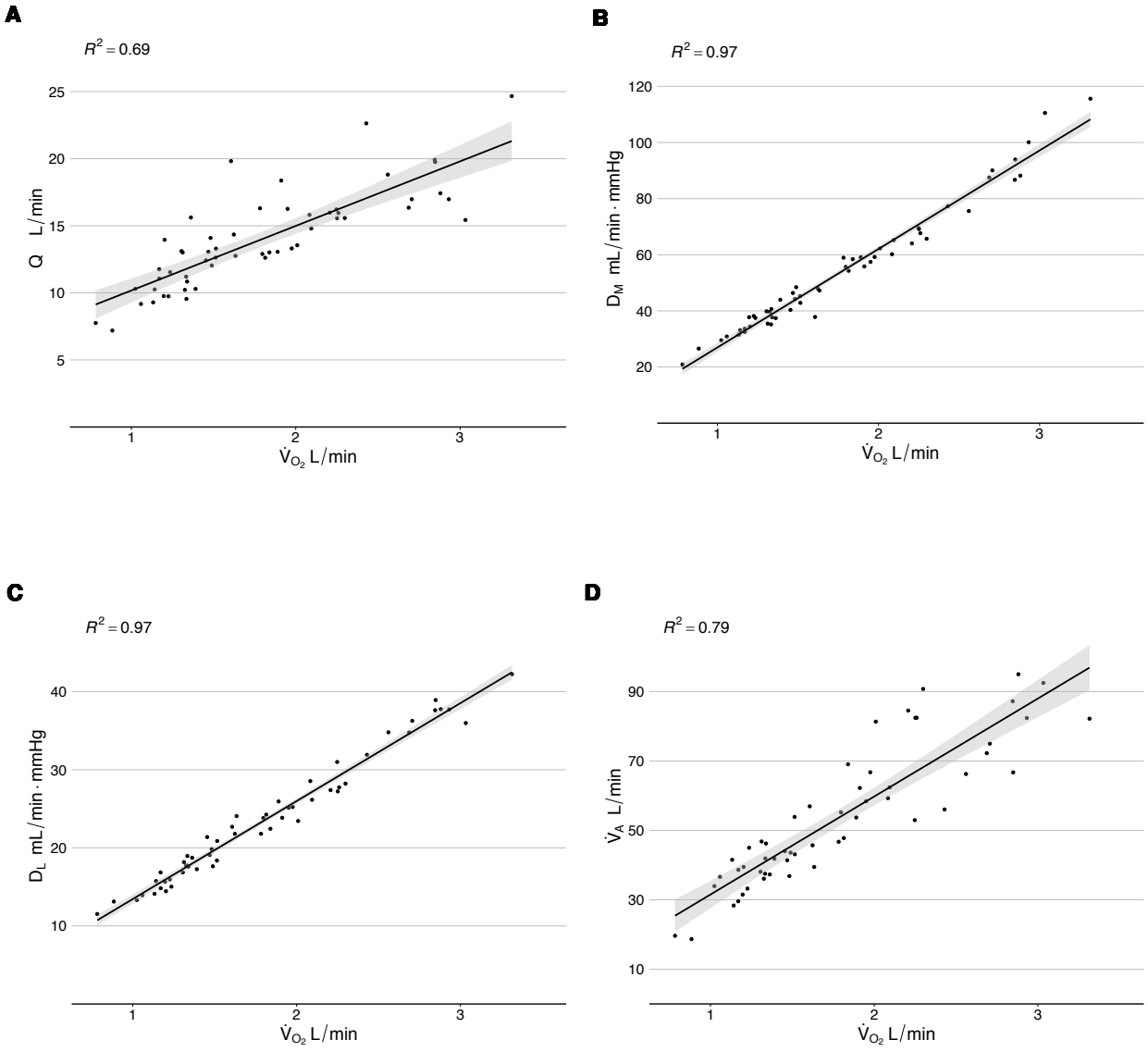

Figure S1. Linear prediction models for reference values of O_2 pathway parameters. **A**, Q vs $\dot{V}_{O_2}$. **B**, D_M vs $\dot{V}_{O_2}$. **C**, D_L vs $\dot{V}_{O_2}$. **D**, $\dot{V}_A$ vs $\dot{V}_{O_2}$. Individual *control* patient data are plotted together with linear models of $Q, D_L, D_M, \text{or } \dot{V}_A$ vs peak $\dot{V}_{O_2}$. Each control individual's O_2 pathway parameters were estimated from their CPET data according to Algorithm 1. R^2 denotes the Pearson correlation coefficient.

We found a strong linear dependence between O_2 pathway parameters $Q, D_L, D_M, \text{or } \dot{V}_A$ and peak $\dot{V}_{O_2}$, among control patients. This offered a natural way to identify reference parameter values for a given HFpEF patient, adjusted to their age,

gender, and body size. First, we determined the patient's age-, gender-, and height-predicted $\dot{V}_{O_2}$. We next used that value together with the above linear models to estimate the patient's reference value for each O_2 pathway parameter (Algorithm 5).

For hemoglobin concentration, we used the reference values of 13.5 mg/dL for women and 15 mg/dL for men.

For v_{max}, we used 1.8*(peak predicted $\dot{V}_{O_2}$) for a reference value, as discussed in section 1.2.

2.3 Peripheral Extraction (ΔAV_{O_2}) in HFpEF: published reports

In Figure 2b we demonstrated that peripheral extraction in HFpEF is impaired. We drew this conclusion from the observation that peak-ΔAV_{O_2} in our HFpEF cohort was smaller than it should have been, given the degree to which cardiac output was reduced relative to controls. We also showed that when the average HFpEF values of ($Q, \Delta AV_{O_2}$) from published reports are plotted on the same graph, $\Delta AV_{O_2}$is consistently reduced relative to our control calibration line (Figure 2c). We should exercise caution when comparing results across studies due to differences in exercise conditions, criteria for defining controls, and methods for determining ΔAV_{O_2} (e.g. measured vs calculated). To mitigate these perils, we recreated Figure 2b for each published study using study-specific data whenever possible. In particular, we used as much control data as was available in each report to construct a study-specific control calibration curve. The Fu et al study[18] did not have a control group with normal exercise capacity, so it does not appear in the figure below.

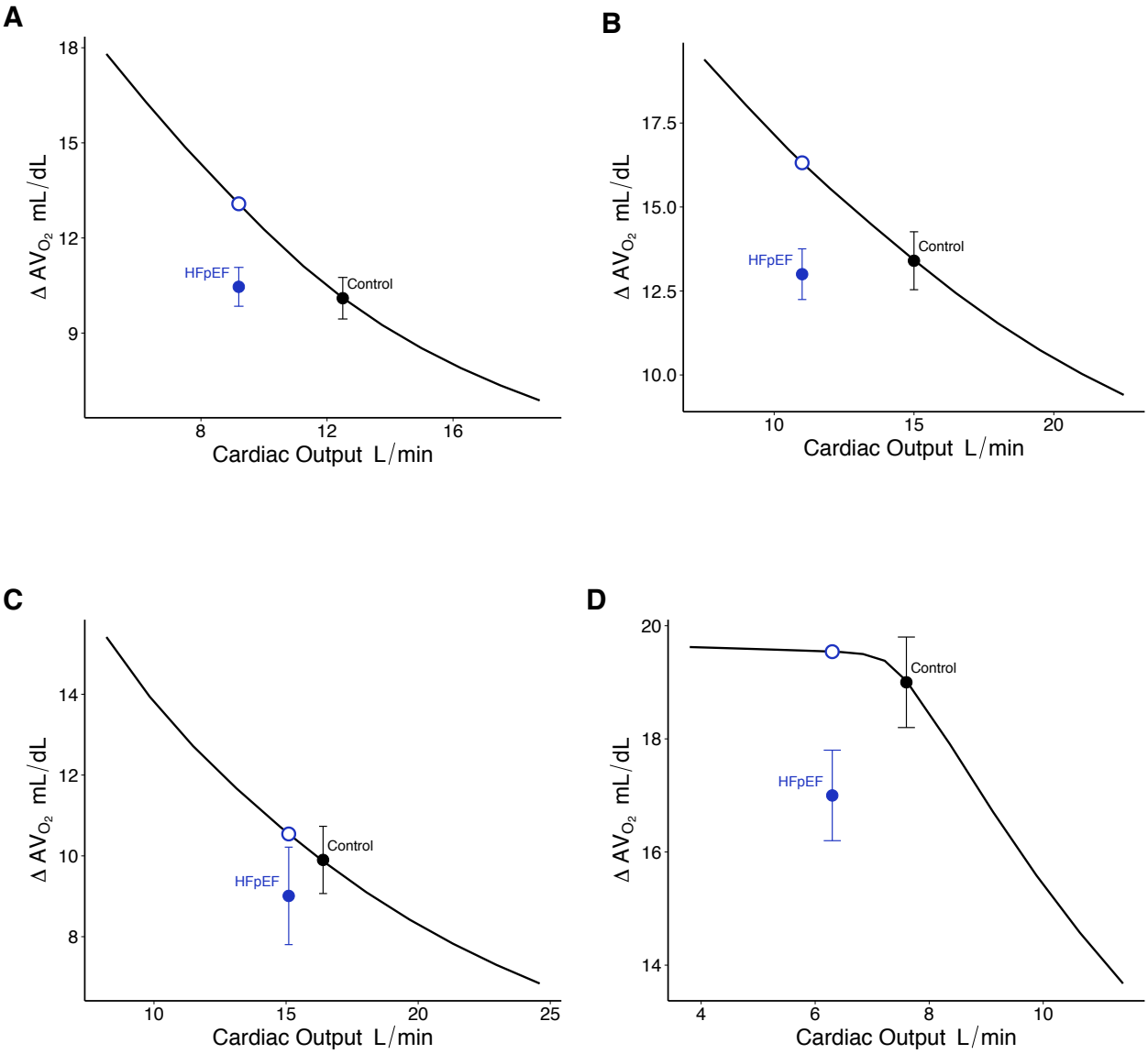
A
B
C
D
Δ AVO2 mL/dL
Cardiac Output L/min
HFpEF
Control

Figure S2. Observed HFpEF ΔAV_{O_2} versus calibrated control ΔAV_{O_2} values from four published HFpEF studies. Filled circles depict the reported mean values of Q and ΔAV_{O_2} for Control (black) and HFpEF (blue) groups at peak exercise. The HFpEF ΔAV_{O_2} values are normalized to the mean hemoglobin reported in the associated control groups. Error bars depict 95% confidence intervals. Each black curve represents the series of ΔAV_{O_2} values predicted at each possible Q, for control individuals. This calibration curve was estimated using Algorithm 4 together with study-specific control group data. Open circles depict the predicted value of control ΔAV_{O_2} at mean HFpEF Q. **A**, Abudiab et al.[19] For these calculations we used the mean control measurements reported from the control group labeled "all patients", with one exception. Peak exercise Pa_{O_2} and $P\bar{v}_{O_2}$ could only be derived from measurements available from "cohort 1". **B**, Santos et al.[20] **C**, Bhella et al.[21] Neither arterial nor venous O_2 levels were reported. To derive the control ΔAV_{O_2} curve we approximated peak exercise Pa_{O_2} by 95mmHg, the mean value observed in our control group. **D**, Haykowsky et al.[22] Neither O_2 levels nor hemoglobin values were reported so we approximated the control peak Pa_{O_2} by 95mmHg, and the hemoglobin by 14 mg/dL in both HFpEF and controls.

By recapitulating the findings of Figure 2c with study-specific control calibration lines, Figure S2 affirms the conclusion that peak-ΔAV_{O_2} in HFpEF is abnormal. The principle at the heart of these analyses is that when cardiac output is reduced, normal peripheral extraction should result in a ΔAV_{O_2} that is *greater* than controls.

2.4 Mitochondrial Respiration: Sensitivity Analysis

The O_2 transport and utilization equations quantify mitochondrial respiration using two parameters, v_{max} and p_{50} (equation 8), that we approximated with reference values. The impact of these approximations on our principal conclusions warrants sensitivity testing. The true parameter values are difficult to measure in the individual patient, and to our knowledge have never been measured directly in vivo, at peak exercise. However, as discussed in Section 1.2, published measurements from both HFrEF patients and controls permit a reasonable, personalized approximation to v_{max} using reference values of mitochondrial respiratory reserve, $R_{mito} = v_{max}/\text{peak}\,\dot{V}_{O_2}$. Our chief assumption in using the reference value for R_{mito} derived from HFrEF patients is that it applies to HFpEF as well. For the p_{50} parameter, measurements have only been reported from mitochondrial preparations ex vivo. We used a fixed normal reference value for p_{50}, 0.24mmHg, for all patients.

To test the sensitivity of our key results to v_{max} and p_{50} approximations, we systematically varied these parameters over a 2-dimensional grid of values. At each

gridpoint we recalculated each HFpEF patient's D_M, VDR_{D_M}, and VDR_Q, and then determined the mean value of these parameters over the group. We used this approach to assess the sensitivity of two principle findings: 1) Impaired skeletal muscle diffusion capacity in HFpEF compared to controls (Figure S3a) and 2) $VDR_{D_M} > VDR_Q$ in HFpEF (Figure S3b). Both of these findings could be sensitive to impaired mitochondrial function (high p_{50}, low v_{max}). To test this, we varied p_{50} from 0.24mmHg to 0.74mmHg, a pathological value reported from Leigh syndrome patients. Rather than vary v_{max}, we varied R_{mito} from 1.05 to 1.25 and then set $v_{max} = R_{mito} * \text{meausured peak } \dot{V}_{O_2}$ for each patient; in the main text calculations for HFpEF we used $R_{mito} = 2.0$ to calculate v_{max} in each HFpEF patient (Section 1.2). The normalized R_{mito} scale lends itself to comparing patients that cover a spectrum of peak $\dot{V}_{O_2}$, and is equivalent to varying v_{max} itself. We note that R_{mito} must be strictly greater than 1 since $\dot{V}_{O_2}$should not exceed v_{max}; nor can $\dot{V}_{O_2}$ equal v_{max}, as such a high rate of O_2 consumption would require an infinite intramitochondrial pO_2 (see equation 8); in fact, simply noting that P_{mito}< venous pO_2 is sufficient to set a loose lower bound on v_{max}.

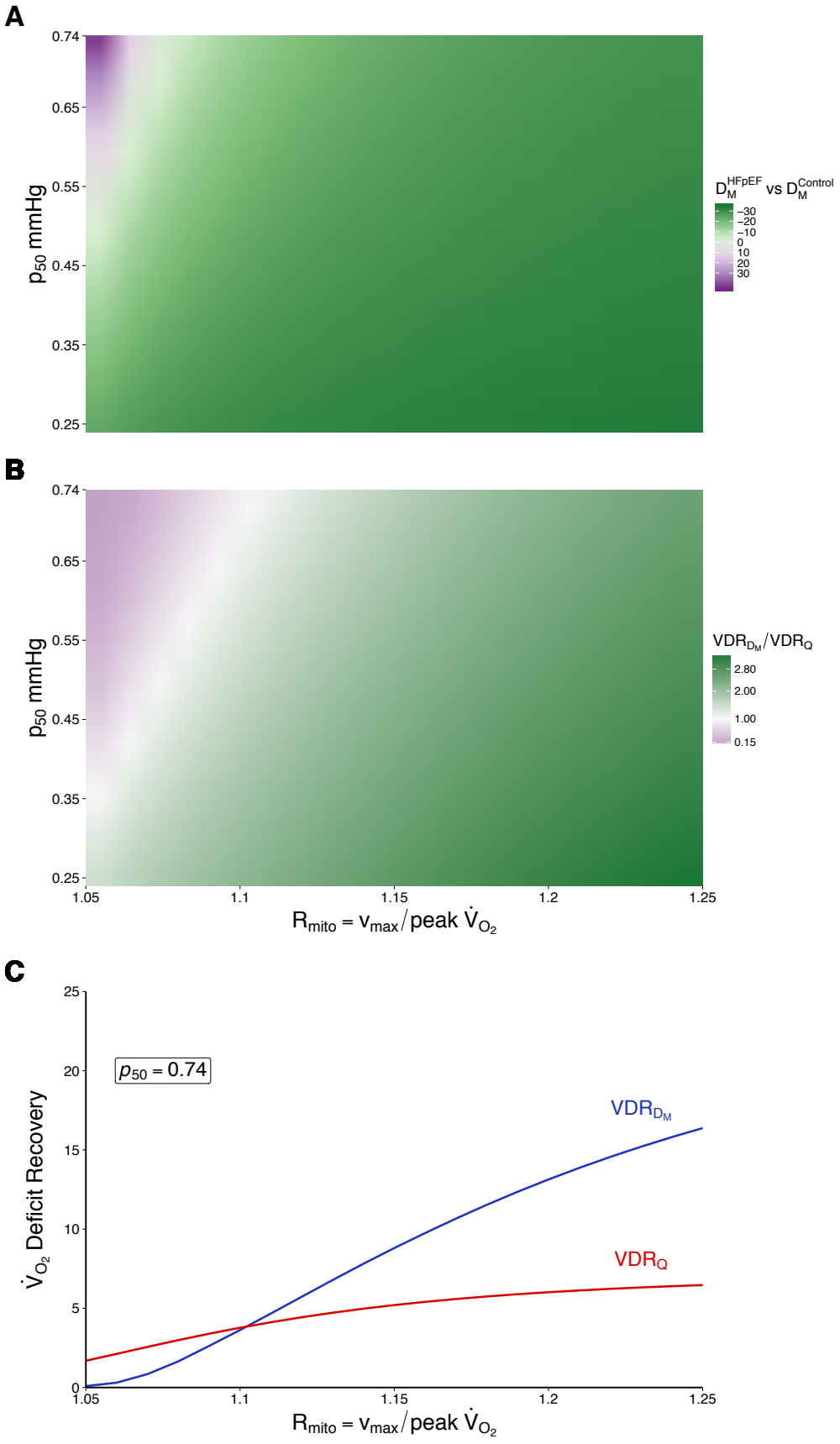
A
0.74
0.65
0.55
0.45
0.35
0.25
p50 mmHg
DMHFpEF vs DMControl
−30
−20
−10
0
10
20
30
B
0.74
0.65
0.55
0.45
0.35
0.25
p50 mmHg
VDRDM/VDRQ
2.80
2.00
1.00
0.15
1.05
1.1
1.15
1.2
1.25
Rmito = vmax/peak V̇O2
C
25
20
15
10
5
0
V̇O2 Deficit Recovery
p50 = 0.74
VDRDM
VDRQ
1.05
1.1
1.15
1.2
1.25
Rmito = vmax/peak V̇O2

Figure S3. Sensitivity of D_M, VDR_{D_M}, VDR_Q to the mitochondrial respiration parameters p_{50} and R_{mito}. **A**, D_M sensitivity analysis. Panel A demonstrates the range of values that mean HFpEF D_M takes relative to control D_M, as p_{50} and R_{mito} are varied over a range of pathologic values. Each point on the grid of p_{50} and R_{mito} values is color coded to reflect the percent difference between mean HFpEF D_M and mean control D_M. Green reflects a reduction in D_M in HFpEF vs controls and purple reflects an increase in D_M vs controls. **B**, VDR_{D_M}, VDR_Q sensitivity analysis. Panel B is constructed analogously to panel A, where the color now reflects the ratio of mean VDR_{D_M} to mean VDR_Q, with the mean taken over HFpEF patients. Green indicates values greater than 1 and purple indicates values less than 1. **C**, VDR_{D_M}, VDR_Q sensitivity analysis for a fixed pathologic value of p_{50}. Panel C shows the absolute value of mean VDR_{D_M} and mean VDR_Q in HFpEF, as a function of R_{mito}, with p_{50} fixed at 0.74 mmHg, the most pathologic value we considered.

The results of this sensitivity analysis demonstrate that our two principal study findings remain valid over the vast majority of pathologic mitochondrial parameter values. First, peripheral diffusion capacity is impaired in HFpEF for all but extreme values of R_{mito} and p_{50}, though the magnitude of the effect varies (Figure S3a), as first theoretically described in Cano et al.[5] Second, the predicted improvement in the $\dot{V}_{O_2}$deficit due to correcting D_M is greater than that due to correcting Q, for all but a small range of severely abnormal mitochondrial parameter values (Figure S3b). While there does exist a small range of R_{mito} where $VDR_{D_M} < VDR_Q$, the actual magnitudes of both VDR_{D_M} and VDR_Q in this range are exceedingly small (Figure S3c). Not surprisingly, when peak $\dot{V}_{O_2}$is within ~10% of v_{max} the dominant limiting parameter is in fact v_{max}, and attempts to improve $\dot{V}_{O_2}$by augmenting O_2 delivery are minimally effective.

2.5 Quantifying the causal impact of an O_2 pathway defect: $\dot{V}_{O_2}$ control coefficients

In addition to the VDR coefficient we evaluated a second metric of the causal impact of an O_2 pathway step on exercise capacity—the "$\dot{V}_{O_2}$control coefficient" (VCC). We borrowed this metric directly from Metabolic Control Theory,[23] where it is known more generally as the flux control coefficient (FCC). We define and illustrate the VCC for cardiac output in Figure S4a. In contrast to the VDR coefficient, which quantifies the $\dot{V}_{O_2}$improvement due to *complete* correction of an O_2 pathway parameter, the VCC quantifies the normalized $\dot{V}_{O_2}$ response to an *incremental* change in the parameter. In particular, it is defined as the % increase in $\dot{V}_{O_2}$ per % increase in an O_2 pathway

parameter, at the measured value of that parameter. We used Algorithm 2 to calculate the $\dot{V}_{O_2}$ response to such an incremental change in Q or D_M, for each HFpEF patient.

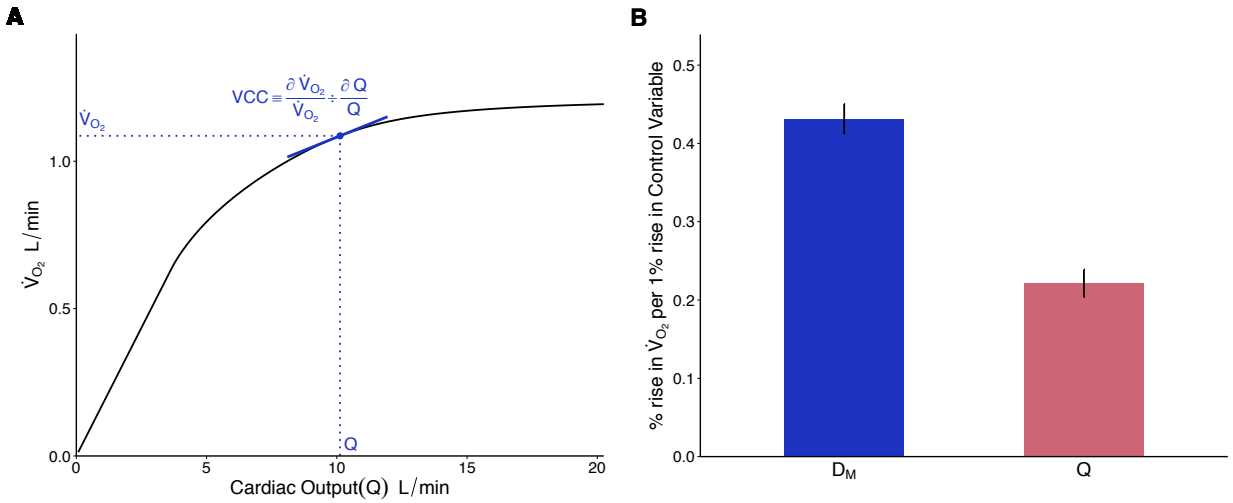

Figure S4. $\dot{V}_{O_2}$ control coefficients (VCC) for D_M and Q in HFpEF. **A**, VCC concept. The VCC is a dimensionless quantity defined as the fractional rise in $\dot{V}_{O_2}$ per fractional rise in a control variable (e.g. Q), where the rise in the control variable is taken relative to its observed (CPET-derived) value. Panel A illustrates the VCC for a typical (median $\dot{V}_{O_2}$) HFpEF patient. The plotted point is the measured value of (Q, $\dot{V}_{O_2}$). **B**, mean VCC_{DM} vs mean VCC_Q in the HFpEF population. Error bars depict 95% confidence intervals. P<0.001 for the difference.

Figure S4b demonstrates that a second metric of causal impact, the VCC, corroborates the findings from our VDR calculations. In particular, peak $\dot{V}_{O_2}$ in HFpEF is predicted to be more responsive to increases in peripheral diffusive delivery of O_2 than it would be to cardiac output.

2.6 Disease Burden: Comorbid O_2 pathway defects

One of the most striking observations from Figure 4c,d is that the maximum VDR among HFpEF patients actually diminishes as the O_2 pathway defect becomes more severe. This counterintuitive finding could be explainable if the 'defect vs VDR' relationship were confounded, in particular by variation in the remaining O_2 pathway defects *not* displayed on the graph. For example, in the HFpEF patients with severe cardiac output defects (Figure 4c, Q-defect > 50%), low cardiac output may not be their only problem—they may also harbor significant defects in the remaining O_2 pathway parameters. Compound disease would be expected to dampen the benefit of correcting cardiac output.

To assess the relationship between one O_2 pathway defect and the remainder, we constructed an O_2 pathway impairment score. To compute a patient's impairment score (formula below), we simply summed the magnitudes of his or her O_2 pathway defects, where a parameter defect is quantified as $1 - \frac{\text{observed value}}{\text{predicted value}}$. Since our goal was to compare the overall pathway impairment with the severity of one specific O_2 pathway defect, we removed the contribution of that O_2 pathway defect from this sum. We did not include a contribution from v_{max} deficits as our approximation to v_{max} depends on peak $\dot{V}_{O_2}$, a variable which is largely accounted for in the score by virtue of the included O_2 pathway parameter terms. As a result, the impairment score gets a contribution from 4 out of the 5 O_2 pathway parameters ($Q, D_L, D_M, Hb, \dot{V}_A$), for a maximum value of 4. For illustration, the formula below describes the impairment score plotted in Figure S5a:

$$Impairment\ Score_{-Q} = 4 - \left(\frac{D_L^{observed}}{D_L^{predicted}} + \frac{D_M^{observed}}{D_M^{predicted}} + \frac{Hb^{observed}}{Hb^{predicted}} + \frac{\dot{V}_A^{observed}}{\dot{V}_A^{predicted}} \right)$$

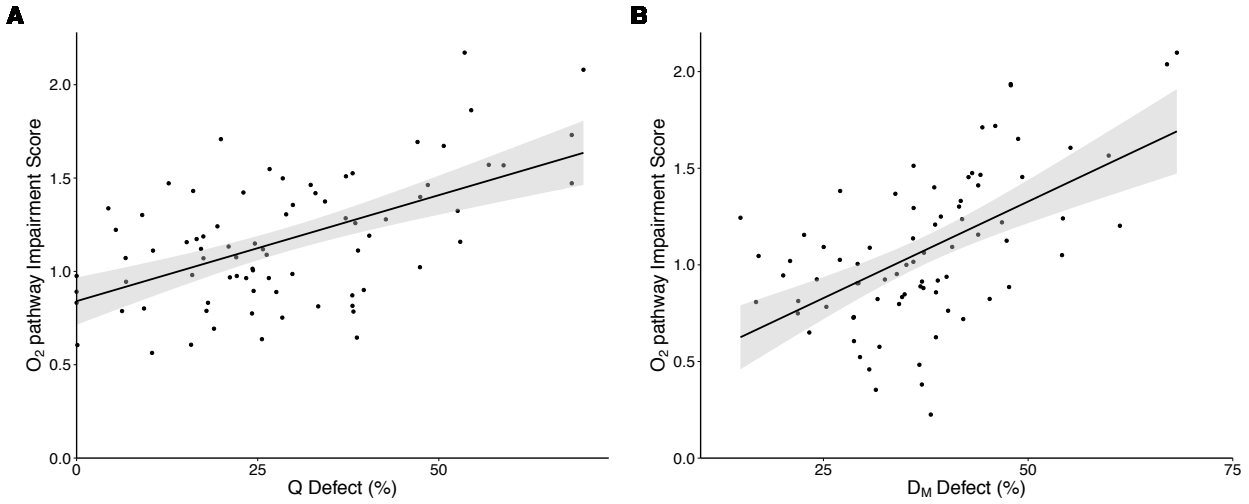

Figure S5. O_2 pathway impairment score (IS) as a function of defects in Q or D_M. Individual HFpEF patients are plotted together with a linear model relating the O_2 pathway defect to the impairment score. **A**, IS_{-Q} vs Q-defect. Panel A shows the relationship of impaired cardiac output to the burden of remaining O_2 pathway defects ($D_L, D_M, Hb, \dot{V}_A$). **B**, IS_{-D_M} vs D_M-defect. Panel B shows the relationship between impaired skeletal muscle diffusion capacity and the burden of remaining O_2 pathway defects ($Q, D_L, Hb, \dot{V}_A$). The shaded grey regions depict 95% confidence regions of the linear models.

Whether patients are indexed by their defect in cardiac output or skeletal muscle diffusion capacity, the severity of one defect predicts pathology in the remaining O_2 pathway steps (Figure S5). This accords with clinical intuition—sick patients are typically burdened by multiple comorbidities. In the context of exercise intolerance, comorbidities can be viewed as accessory defects in distinct steps of the O_2 pathway. These results, together with Figure 4cd, lend quantitative causal support to another common observation: when selecting patients for therapy, there is often a sweet-spot of disease severity—enough pathology that treatment could result in meaningful improvement, but not so much that the burden of disease will permit only vanishing therapeutic returns.

3. References:

1. Lewis GD, Lachmann J, Camuso J, Lepore JJ, Shin J, Martinovic ME, Systrom DM, Bloch KD and Semigran MJ. Sildenafil improves exercise hemodynamics and oxygen uptake in patients with systolic heart failure. *Circulation*. 2007;115:59-66.
2. Borlaug BA, Melenovsky V, Russell SD, Kessler K, Pacak K, Becker LC and Kass DA. Impaired chronotropic and vasodilator reserves limit exercise capacity in patients with heart failure and a preserved ejection fraction. *Circulation*. 2006;114:2138-2147.
3. Franciosa JA, Leddy CL, Wilen M and Schwartz DE. Relation between hemodynamic and ventilatory responses in determining exercise capacity in severe congestive heart failure. *Am J Cardiol*. 1984;53:127-134.
4. Wagner PD. A theoretical analysis of factors determining VO2 MAX at sea level and altitude. *Respir Physiol*. 1996;106:329-343.
5. Cano I, Mickael M, Gomez-Cabrero D, Tegner J, Roca J and Wagner PD. Importance of mitochondrial P(O2) in maximal O2 transport and utilization: a theoretical analysis. *Respir Physiol Neurobiol*. 2013;189:477-483.
6. Wagner PD. Modeling O(2) transport as an integrated system limiting (.)V(O(2)MAX). *Comput Methods Programs Biomed*. 2011;101:109-114.
7. Ben-Tal A. Simplified models for gas exchange in the human lungs. *J Theor Biol*. 2006;238:474-495.
8. Keener JP, Sneyd J and SpringerLink (Online service). Mathematical physiology. *Interdisciplinary applied mathematics 8*. 2009:2 v.
9. Scandurra FM and Gnaiger E. Cell respiration under hypoxia: facts and artefacts in mitochondrial oxygen kinetics. *Adv Exp Med Biol*. 2010;662:7-25.
10. Dash RK and Bassingthwaighte JB. Blood HbO2 and HbCO2 dissociation curves at varied O2, CO2, pH, 2,3-DPG and temperature levels. *Ann Biomed Eng*. 2004;32:1676-1693.
11. Esposito F, Mathieu-Costello O, Shabetai R, Wagner PD and Richardson RS. Limited maximal exercise capacity in patients with chronic heart failure: partitioning the contributors. *J Am Coll Cardiol*. 2010;55:1945-1954.
12. Hundley WG, Bayram E, Hamilton CA, Hamilton EA, Morgan TM, Darty SN, Stewart KP, Link KM, Herrington DM and Kitzman DW. Leg flow-mediated arterial dilation in elderly patients with heart failure and normal left ventricular ejection fraction. *Am J Physiol Heart Circ Physiol*. 2007;292:H1427-1434.
13. Richardson RS, Noyszewski EA, Kendrick KF, Leigh JS and Wagner PD. Myoglobin O2 desaturation during exercise. Evidence of limited O2 transport. *J Clin Invest*. 1995;96:1916-1926.
14. Pecina P, Gnaiger E, Zeman J, Pronicka E and Houstek J. Decreased affinity for oxygen of cytochrome-c oxidase in Leigh syndrome caused by SURF1 mutations. *Am J Physiol Cell Physiol*. 2004;287:C1384-1388.
15. Boushel R, Gnaiger E, Calbet JA, Gonzalez-Alonso J, Wright-Paradis C, Sondergaard H, Ara I, Helge JW and Saltin B. Muscle mitochondrial capacity exceeds maximal oxygen delivery in humans. *Mitochondrion*. 2011;11:303-307.
16. Mettauer B, Zoll J, Sanchez H, Lampert E, Ribera F, Veksler V, Bigard X, Mateo P, Epailly E, Lonsdorfer J and Ventura-Clapier R. Oxidative capacity of skeletal muscle in heart failure patients versus sedentary or active control subjects. *J Am Coll Cardiol*. 2001;38:947-954.
17. Jones NL. *Clinical exercise testing*. 3rd ed. Philadelphia: Saunders; 1988.
18. Fu TC, Yang NI, Wang CH, Cherng WJ, Chou SL, Pan TL and Wang JS. Aerobic Interval Training Elicits Different Hemodynamic Adaptations Between Heart Failure Patients with Preserved and Reduced Ejection Fraction. *Am J Phys Med Rehabil*. 2016;95:15-27.
19. Abudiab MM, Redfield MM, Melenovsky V, Olson TP, Kass DA, Johnson BD and Borlaug BA. Cardiac output response to exercise in relation to metabolic demand in heart failure with preserved ejection fraction. *Eur J Heart Fail*. 2013;15:776-785.
20. Santos M, Opotowsky AR, Shah AM, Tracy J, Waxman AB and Systrom DM. Central cardiac limit to aerobic capacity in patients with exertional pulmonary venous hypertension: implications for heart failure with preserved ejection fraction. *Circ Heart Fail*. 2015;8:278-285.
21. Bhella PS, Prasad A, Heinicke K, Hastings JL, Arbab-Zadeh A, Adams-Huet B, Pacini EL, Shibata S, Palmer MD, Newcomer BR and Levine BD. Abnormal haemodynamic response to exercise in heart failure with preserved ejection fraction. *Eur J Heart Fail*. 2011;13:1296-1304.

22. Haykowsky MJ, Brubaker PH, John JM, Stewart KP, Morgan TM and Kitzman DW. Determinants of exercise intolerance in elderly heart failure patients with preserved ejection fraction. *J Am Coll Cardiol*. 2011;58:265-274.
23. Fell D. *Understanding the control of metabolism.* 1st ed. London ; Miami
Brookfield, VT: Portland Press ;
Distributed by Ashgate Pub. Co. in North America; 1997.